ABSTRACT

FUNCTIONALIZATION OF NANOCLAYS THROUGH EXCHANGE REACTIONS

by

Jin Uk Ha

A cationic clay (sodium-montmorillonite, MMT) and an anionic clay (hydrotalcite, HT) were treated with two phosphonium based ionic liquids (ILs) and a commercial corrosion inhibitor. Clay modification was examined by TGA, FTIR and WXRD. The cationic clay modified with both ILs had similar thermal stabilities since they contained the same cation although the original anions were different. The thermal stability of the modified clays was higher than that of a commercial organoclay and of clays modified in our group with smaller MW pyridinium and imidazolium based cations. 10 wt% of interchanged cation was found under selected time/temperature treatment conditions.

Clays modified with the long chain phosphonium based ILs showed excellent dispersion in a PP matrix, by contrast to the poor dispersion of clays modified with smaller MW imidazolium and pyridinium cations.

MMT was also modified with a cationic corrosion inhibitor. FTIR, TGA, WXRD results suggest intercalation with its cation. Accelerated corrosion tests on steel panels coated with a paint containing MMT/inhibitor combinations showed better protection than paints containing either clay or corrosion inhibitor.

By contrast to the cationic clay, attempts to intercalate a large organic anion from [THTDP][DE] were not successful, as suggested by WXRD data. Possible reasons are provided.

FUNCTIONALIZATION OF NANOCLAYS THROUGH EXCHANGE REACTIONS

by
Jin Uk Ha

A Thesis
Submitted to the Faculty of
New Jersey Institute of Technology
in Partial Fulfillment of the Requirements for the Degree of
Master of Science in Chemical Engineering

Otto H. York Department of Chemical Engineering

January 2007

APPROVAL PAGE

FUNCTIONALIZATION OF NANOCLAYS THROUGH EXCHANGE REACTIONS

Jin Uk Ha

Dr. Marino Xanthos, Thesis Advisor — Date
Professor of Chemical Engineering, NJIT

Dr. Kun Sup Hyun, Committee Member — Date
Research Professor of Chemical Engineering, NJIT

Dr. Sanjay V. Malhotra, Committee Member — Date
Assistant Professor of Chemistry and Environmental Science, NJIT

BIOGRAPHICAL SKETCH

Author: Jin Uk Ha

Degree: Master of Science

Date: January 2007

Undergraduate and Graduate Education:

- Master of Science in Chemical Engineering,
  New Jersey Institute of Technology, Newark, NJ, 2007

- Bachelor of Science in Chemical Engineering,
  Inha University, Incheon, Republic of Korea, 2004

Major: Chemical Engineering

Presentations and Publications:

Ha, J. U.; Kim M.; Lee, J.; Choe, S.; Cheong, I. W.; Shim, S. E.
"A Novel Synthesis of Polymer Brush on Multiwall Carbon Nanotubes Bearing Terminal Monomeric Unit" *J. Polym. Sci. A: Polym. Chem* **2006** *44*, 6394-6401.

Lee, J.; Ha, J. U.; Choe, S.; Lee C. S.; Shim S. E.
"Synthesis of Highly Monodisperse Polystyrene Microspheres via Dispersion Polymerization using an Amphoteric Initiator" *J. Colloid Interface Sci.* **2006** *298*, 663-671.

In God I Trust

ACKNOWLEDGMENTS

First and foremost, I wish to express my deepest appreciation to my advisor, Professor Marino Xanthos, not only for his professional advice but also his encouragement, patience and support throughout this research. It was a great honor to have him as my advisor.

I would like to thank my Committee members, Professor K. S. Hyun and Professor S. Malhotra for agreeing to be part of my work. I appreciate their priceless support.

I would also like to thank the staff of the Polymer Processing Institute (PPI), Newark, NJ for providing a friendly and productive environment. Their invaluable cooperation and advice is greatly appreciated.

In addition, I would like to thank Mr. Kuan Yin Lin of NJIT for his help with the SEM and Mr. Neung Hyun Kim currently at Samyang Corporation for providing guidance in planning my experiments. Also, Mr. Jeongwoo Lee of Inha University for providing TEM images and Ms. Georgia Chouzouri of NJIT for her timely support and assistance with WXRD. I would like to thank Mr. Kuil Park, Ms. Laila, Mr. Praveen and Ms. Quyuan Zhou of NJIT as well.

I would like to express my gratitude to Professor Sang Eun Shim of Inha University in Incheon, S. Korea, for showing me the future.

Lastly, I take this opportunity to sincerely thank my father, mother, my beloved daughter, Noel Songju, and my companion for life, Hee Jun Kim for their patience, understanding and endless support.

TABLE OF CONTENTS

TABLE OF CONTENTS
(Continued)

TABLE OF CONTENTS
(Continued)

LIST OF TABLES

LIST OF FIGURES

LIST OF FIGURES
(Continued)

Figure **Page**

LIST OF FIGURES
(Continued)

CHAPTER 1

INTRODUCTION

1.1 Objectives

An objective of this research is to modify cationic and anionic clays through ion exchange with a) phosphonium based ionic liquids ([THTDP][DE] and [THTDP][BF_4]) which have different chemical structures and b) a cationic corrosion inhibitor (Halox® 520). An additional objective is the comparison of the montmorillonite and hydrotalcite clays, which were modified with ionic liquids [THTDP][DE] and [THTDP][BF_4], with nanoclays which were previously modified with lower molecular weight ionic liquids and also with a commercial nanoclay (Cloisite® 15A). Modified montmorillonite with Halox® 520 was used as a corrosion inhibitor in accelerated corrosion tests and compared with neat Halox® 520.

Modified clays with ionic liquids and Halox® 520 were characterized by Thermogravimetric Analysis (TGA), Fourier Transform Infrared Spectroscopy (FTIR), Wide Angle X-ray Diffraction (WXRD), Scanning Electron Microscopy (SEM), and Transmission Electron Microscopy (TEM) and compared with unmodified clays. Modified clays were also incorporated into polypropylene (PP) in order to evaluate their degree of intercalation and extent of dispersion in polymer matrix and in a protective coating applied on metallic substrates.

The objective of the latter series of experiments was to evaluate the possibility of enhancing corrosion protection through combinations of impermeable platey nanoclays with corrosion inhibitiors.

1.2 Ionic Liquids

1.2.1 General

Ionic liquids (ILs) are organic salts with low melting points typically below 100 °C. They usually consist of nitrogen or phosphorous containing organic cations and anions such as halides, tetrafluoroborate and hexafluorophosphates (Zhu 2006). ILs have novel solvent properties featuring non volatility, non flammability, thermal stability, and a wide liquid temperature range; they have been investigated for not only organic synthesis, but also other processes such as bio-processing operations, catalysts, gas separation, as electrolytes in electrochemistry and so on (Zhao and Malhotra 2002).

Ionic liquids are comprised only of ions and can be produced with a variety of cations and anions as shown in Figures 1.1 and 1.2. Imidazolium and pyridinium are the most common organic cations, but phosphonium and ammonium based ILs have been investigated. BF_4^-, PF_6^-, $CH_3CO_2^-$, NO_2^-, etc. are commonly found anions in ionic liquids [Kim et al. 2006].

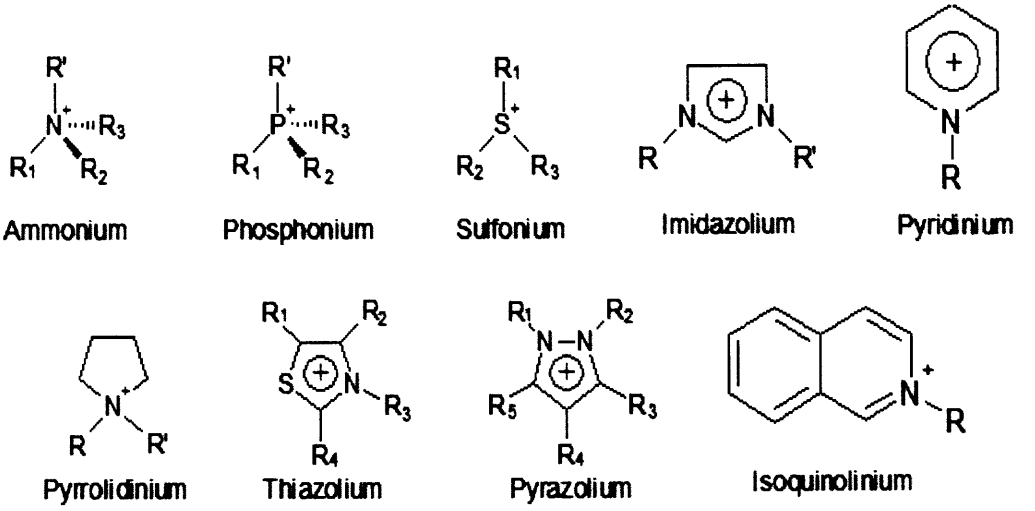

Figure 1.1 Common types of cations in ionic liquids.
(Source: Xanthos, M. "Novel Functionalization Routes for Nanoclays", Functional Filler, 2006 Conf., Proc., Atlanta, GA, Sep. 25 – 27).

$AlCl^{4-}$	$(CF_3SO_2)_2N^-$	HSO_4^-
$AuCl_4^-$	$CF_3SO_3^-$	I^-
$B(Et_3Hex)^-$	$(CN)_2N^-$	NO_2^-
BF_4^-	Cl^-	NO_3^-
Br^-	$CH_3CO_2^-$	PF_6^-
$CF_3CO_2^-$	$GaCl_4^-$	SbF_6^-
$n\text{-}C_8H_{17}OSO_3^-$	Carborane anions $(1\text{-}R\text{-}CB_{11}H_6X_6)^-$	

Figure 1.2 Commonly used anions in ionic liquids.
(Source: Xanthos, M. "Novel Functionalization Routes for Nanoclays", Functional Filler, 2006 Conf., Proc., Atlanta, GA, Sep. 25 – 27).

While a great attention has been given to quaternary nitrogen based ionic liquids (e.g., ammonium, imidazolium, pyridinium, etc) in recent years, specific accounts of ionic liquids containing quaternary phosphorus cations have been less common [Gordon et al. 2001]. However, phosphonium based ionic liquids have been shown to have better properties than nitrogen based ionic liquids, especially thermal properties [Bonnet et al. 2006, Stoeffler et al. 2006]. The decomposition point of phosphonium ionic liquids on heating varies depending on the anion; thermal analysis indicates a thermal stability over of 300°C for many species [Bradaric et al. 2002]. Hence, research on nanoclay composites containing clay modified with phosphonium based ionic liquids has increased due to the better thermal stability of phosphonium based ionic liquids. [Snedden et al. 2003; Stoeffler et al. 2006; Byrne et al. 2005].

1.2.2 Properties of Ionic Liquids

Polarities are commonly applied for solvent classification. Generally, ionic liquids are regarded as a polar solvent. However, unlike conventional solvents, ionic liquids are

complex solvents with many types of solvent-solute interactions including hydrogen bonding, π-π bonding, ionic bonding, etc [Zhu 2006]. Due to the complexities of ionic liquids, they show remarkable differences from conventional solvents having similar polarity.

Ionic liquids have no measurable vapor pressure unlike volatile organic solvents and extraction media. Therefore, there is no loss of solvent through evaporation. Due to the properties of ILs, they have often been discussed as green solvents since environmental and safety problems arising through the use of volatile organic solvents can be avoided by the use of the non volatile IL reaction media [Chiappen et al. 2004].

According to Ngo et al. (2000), cations of ILs do not affect much their thermal stability, but anions of ILs decrease thermal stability on decomposition as hydrophilicity increases; the thermal stability of ionic liquids relies on the anions as shown below (in case of imidazolium based ionic liquids):

$$[PF_6]^- > [Tf_2N]^- \sim [BF_4]^- > \text{halides}$$

The high viscosity of some ionic liquids is one of the largest barriers for their applications because it may create a reduction in the rate of many organic reactions and in the diffusion rate of redox species. It has been reported that the structure of anions decreases the viscosity of ionic liquids in the following order [Huddleston et al. 2001]:

$$[Tf_2N]^- < [CF_3SO_3]^- < [BF_4]^- < [SbF_6]^- < [PF_6]^- < [Cl]^-$$

Ionic liquids normally have higher viscosity than water. The viscosity of ILs decreases with increasing temperature. The viscosity of ionic liquids often follows either an Arrhenius behavior or the Vogel-Tammann-Fulcher (VFT) equation. The Arrhenius model can describe the ionic liquids that contain less symmetrical cations without

functional groups in the alkyl chain; on the other hand, the VTF equation can be used for ionic liquids that contain small and symmetrical cations with low molar mass. However, there are still other types of ionic liquids, whose viscosity can not be predicted by those models due to their complex structure [Calrol 2003, Zhu 2006, Xu et al 2003].

1.2 Functional Fillers

1.3.1 General

Fillers are materials which can be added to polymers in small quantity to enhance their properties. Their major contribution is, not only improving the properties of the polymers, but also cost saving by replacing the usually more expensive polymer [Xanthos et al. 2005].

Modified polymers containing high aspect ratio fillers, exhibit enhanced properties over unfilled polymers, such as higher modulus, reduced water and gas permeability, improved solvent resistance, enhanced conductivity, improved UV absorption and scratch resistance. Furthermore, mechanical performance, ablation performance, thermal stability, and flame retardancy may also be improved [Gopakumar et al. 2006, Giannelis et al. 2002, Xanthos et al. 2005]. Due to nanometer size dispersion of nanofunctional fillers in the polymer matrix, nanocomposites generally exhibit improvements in the properties of polymeric materials at very low volume loadings (1~5%) compared to conventional higher volume loadings (30~50%) of macro-size filler in conventional composites [Gopakumar et al. 2006].

1.3.2 Classification and Types of Fillers

Fillers can be categorized into either organic or inorganic. Furthermore, they can be subdivided according to their chemical family (Table 1.1), shape and size, or aspect ratio (Table 1.2). Industrial minerals such as talc, calcium carbonate, mica, kaolin, wollastonite and barite are the most generally used fillers [Xanthos et al. 2005].

Table 1.1 Chemical Families of Fillers for Plastics

Chemical Family		Example
In-organic	Oxides	Glass, MgO, SiO_2, Sb_2O_3, Al_2O_3
	Hydroxides	$Al(OH)_3$, $Mg(OH)_2$
	Salts	$CaCO_3$, $BaSO_4$, $CaSO_4$, Phosphates
	Silicates	Talc, mica, kaolin, wollastonite, montmorillonite, nanoclays, feldspar, asbestos
	Metals	Boron, Steel
Organic	Carbon, graphite	Carbon fibers, graphite fibers and flakes, carbon nanotubes, carbon black
	Natural polymers	Cellulose fibers, wood flour and fibers, flax, cotton, sisal starch

(Source: Xanthos, M. "Polymers and Fillers", Functional Fillers for Plastics, ed. Xanthos, M., Wiley-VCH, Weinheim: Germany 2005, p 12)

Table 1.2 Particle Morphology of Fillers

Shape	Aspect ratio	Examples
Cube	1	Feldspar, Calcite
Sphere	1	Glass spheres
Block	1-4	Quartz, calcite, silica, barite
Plate	4-30	Kaolin, talc, hydrous alumina
Flake	$50\text{-}200_{++}$	Mica, graphite, monmorillonite nanoclays
Fiber	$20\text{-}200_{++}$	Wollastonite, glass fibers, carbon nanotubes, wood fibers, asbestos fibers, carbon fibers

(Source: Source: Xanthos, M. "Polymers and Fillers", Functional Fillers for Plastics, ed. Xanthos, M., Wiley-VCH, Weinheim: Germany 2005, p 13)

1.3.3 Nanoclays

Clays are the most common minerals on the earth's surface. They are very versatile materials that are used in many different areas such as building materials, ceramics, paper coatings, pharmaceuticals, adsorbents, ion exchangers, etc. [Vaccari 1998].

When a clay mineral is a phyllosilicate with a sheet structure having thickness in the order of 1 nm and surfaces of around 50 – 150 nm in one dimension, it is generally referred to as nanoclay. The mineral base of clays is hydrophilic and it can be natural or synthetic. Cationic clays are widespread in nature, whereas anionic clays are rarer in nature but relatively simple and inexpensive to synthesize. The clay surface can be changed into organophilic by chemical modification. Therefore, it can be compatible with organic polymers. Nanocomposite is the term generally applied when large surface area of nanoclays ($750 m^2/g$) are added to a host polymer [Kamena 2005].

According to Grim (1962), clay materials essentially consist of extremely tiny crystalline particles of one or more members of a small group of minerals that are known as clay minerals. These minerals are essentially hydrous aluminum silicates, with magnesium or entirely iron proxying or in part for the aluminum in some minerals; some clays contain alkalies or alkaline earth elements as essential constituents. Clay materials contain not only clay minerals but also various non-clay minerals, such as quartz, calcite, feldspar, and pyrite. Many clay materials contain organic material and water-soluble salts as well [Grim 1962].

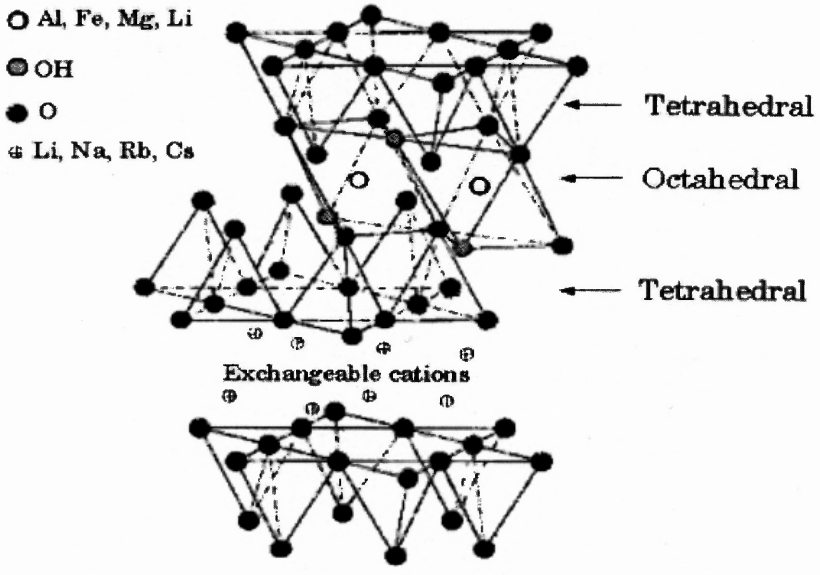

Figure 1.3 Structure of 2:1 phyllosilicate.
(Source: Alexandre et al. *Mater. Sci. Eng.* **2000**, 28, 1-63)

Clay minerals generally consist of two types of structures: octahedral and tetrahedral. Octahedral units contain two sheets of closely packed oxygens or hydroxyls in which aluminum, iron, or magnesium atoms are embedded in octahedral coordination, so that they are equidistant from six oxygens or hydroxyls. If aluminum is present, only 67 % of the possible positions are filled to balance the structure which is the gibbsite structure and has the formula $Al_2(OH)_6$. If magnesium is present, 100% of the possible positions are filled to balance the structure, which is the brucite structure and has the formula $Mg_3(OH)_6$. The tetrahedral unit is made of silica tetrahedra. In each tetrahedral unit, four oxygen atoms or hydroxyls are surrounding a silicon atom and linked by covalent bonding of equal length. The tetrahedral groups can be arranged to form a hexagonal network, which is repeated indefinitely to form a sheet of composition $Si_4O_6(OH)_4$. Generally, the clays used in nanocomposites are normally 2:1 phyllosilicates as shown in Figure 1.3 where the octahedral structure is surrounded by two tetrahedral

structures. Clays can be also categorized into several sub-groups based on their electrical charge, chemical structure, and composition. [Carrado, 2004; Grim, 1962].

Clay minerals are able to sorb certain anions and cations and retain them in an interchangeable status, in which they can exchange for other anions or cations by treatment with ions in a solution (the exchange reaction also takes place sometimes in a non-aqueous environment). The exchange reactions are stoichiometric and the exchange capacities are generally measured in terms of milliequivalents per gram or more frequently per 100 grams [Grim 1962]. The importance of ion exchange is that the exchangeable ion may influence the physical properties of the material.

1.3.3.1 Cation Exchange of Nanoclays. The cationic clays have negatively charged alumino silicate layers, which have cations in the interlayer space to balance the charge [Reichle, 1986]. Not only clay minerals, but also all extremely fine inorganic materials, have a cation exchange capacity which results from broken bonds around their edges. This capacity increases as the particle size decreases. Cationic clays, with a cation exchange capacity, contain many aluminum silicates such as montmorillonite, vermiculite, smectite, and swelling mica. These clays can be obtained from nature but are difficult to synthesize. [Choy and Park, 2004]. The range of the cation exchange capacity of the clay minerals is listed in Table 1-3.

Table 1.3 Cation Exchange Capacities of Clays at pH 7 (in miliequivalents / 100g)

Materials	Capacity
Kaolinite	3-15
Halloysite $2H_2O$	5-10
Halloysite $4H_2O$	10-40
Montmorillonite	80-150
Illite	10-40
Vermiculite	100-150
Chlorite	10-40
Sepiolite-Attapulgite	20-30

(Source: Grim, R.E. "Ion Exchange and Sorption" Clay Mineralogy, McGraw-Hill, NY **1968** p189.)

There are three main causes of cation exchange capacity of the clay minerals [Grim 1962]:

1. Unsatisfied charges which can be balanced by adsorbed cations would be created by broken bonds near the edges of the silica alumina units. Thus the cation exchange capacity would increase as the number of broken bonds increases and the particle size decreases. The exchangeable cations are held around the edges of the flakes.

2. Substitution within the lattice of trivalent aluminum for quadrivalent silicon in the tetrahedral sheet and lower valence of ions, particularly magnesium, for trivalent aluminum in the octahedral sheet result in unbalanced charges in the structural units of some of the clay minerals. In montmorillonite and vermiculite substitutions within the lattice cause about 80% of the total cation exchange capacity. The cations are held mostly on the basal plane surfaces.

3. The hydrogen of exposed hydroxyl groups would be replaced by cationic exchange.

1.3.3.2 Anion exchange of Nanoclays. Anionic clays have positively charged metal hydroxide layers with balancing anions and water molecules located interstitially; they occur as a natural mineral and can be synthesized by reacting dilute aqueous solutions of magnesium and aluminum chlorides with sodium carbonate (in the case of hydrotalcite) [Reichle 1986 and Newman 1998].

Several names according to their composition and polytype form of the minerals are shown at Table 1.4. [Vaccari 1998].

Table 1.4 Composition, Crystallographic and Symmetry for Some Natural Anionic Clays

Mineral	Chemical composition	Unit cell parameters		Symmetry
		a (nm)	c (nm)	
Hydrotalcite	$Mg_6Al_2(OH)_{16}CO_3 \cdot 4H_2O$	0.3054	2.281	3R
Manasseite	$Mg_6Al_2(OH)_{16}CO_3 \cdot 4H_2O$	0.310	1.56	2H
Pyroaurite	$Mg_6Fe_2(OH)_{16}CO_3 \cdot 4H_2O$	0.3109	2.341	3R
Stichtite	$Mg_6Cr_2(OH)_{16}CO_3 \cdot 4H_2O$	0.310	2.34	3R
Barbertonite	$Mg_6Cr_2(OH)_{16}CO_3 \cdot 4H_2O$	0.310	1.56	2H
Takovite	$Ni_6Al_2(OH)_{16}CO_3 \cdot 4H_2O$	0.3025	2.259	3R
Reevesite	$Ni_6Fe_2(OH)_{16}CO_3 \cdot 4H_2O$	0.3081	2.305	3R
Coalingite	$Mg_{10}Fe_2(OH)_{24}CO_3 \cdot 2H_2O$	0.312	3.75	3R

3R and 2H : Rhombohedral and Hexagonal stacking sequence (three layers polytype and two layers polytype)
a : cation-cation distance within a layer
c : basal distance between two layers
(Source: Drits V. A. et al. *Clays Clay Miner* **1987**, *35*, 401)

Two different stacking sequences are exhibited for hydroxyl sheets of anionic clays, which are rhombohedral and hexagonal. Anionic clays obtained by low temperature synthesis have normally the rhombohedral stacking sequence; hexagonal stacking sequences generally form at higher temperatures.

Anionic clays can also be defined by their chemical composition, basal spacing and stacking sequence. The general formula to describe the chemical composition is shown in Equation 1.1 where M = metal, A = interlayer anion, and b = x or 2x-1 for z = 2 or 1, respectively [Vaccari 1998].

$$\left[M^{z+}_{1-x}M^{3+}_{x}(OH)_2\right]^{b+}\left[A^{n-}_{b/n}\right]mH_2O \qquad (1.1)$$

The replacement of divalent inorganic cations (Mg^{2+}, Ni^{2+} or Zn^{2+}) by trivalent inorganic cations such as Al^{3+} results in an excess of positive charge in the octahedral hydroxide layer; those cations are surrounded by six OH^- ions and the different octahedral share edges to form infinite sheets. The sheets are stacked one on top of the other and are held together by weak hydrogen bonding. The exchangeable interlamellar anion compensates this excess positive charge of the crystal. The amount of exchangeable anion is defined as the anion exchange capacity and determines the interlayer distance [Kim 2006, Reichle 1986]. The structure of hydrotalcite like materials is shown at Figure 1.4

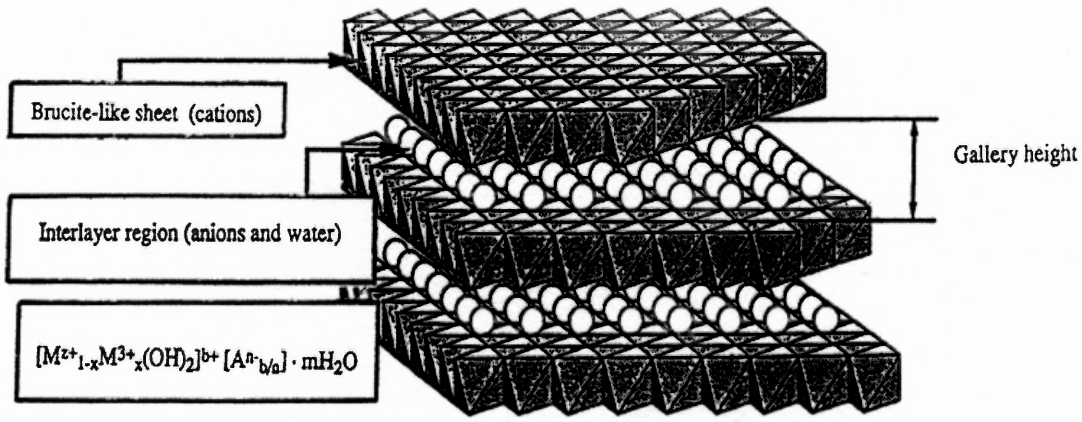

Figure 1.4 Structure of hydrotalcite like material.
(Source: Vaccari, A. *Catal. Today*, **1998**, 41, 53-71).

There are several factors that affect the structures of synthetic anionic clays (ratio of the cations, type of charge balancing anions, crystal morphology, and so on). These are listed in Table 1.5. By controlling these factors, it is possible to produce tailored materials for specific requirements.

Table 1.5 Factors Influencing the Synthesis of Anionic Clays

Structure variables	Preparation variables
Cation size	pH
x value	Precipitation method
Cation stereochemistry	Reagent concentration
Cation mixture	Temperature and aging
Nature of the anion	Washing and drying
	Presence of impurities

(Source: Cavani, F. et al "Hydrotalcite-type anionic clays: Preparation, properties and applications" *Catalysis Today*, **2001**, 11, 173-301)

1.4 Polymer Nanoclay Composites

The first concept of nanocomposite was created by Unitika Ltd. in 1970s (Fujiwara et al. 1976) and developed by Toyota Central Research and Development Laboratories in the late 1980s [Kato et al. 2000]. The concept was that if nanoclays could be fully dispersed or exfoliated in polymers at relatively low weight contents (2 - 5 wt %), mechanical and barrier properties should be improved.

1.4.1 The Structure of Nanocomposites

Three types of composite morphology can be observed when nanoclays are dispersed in a polymer matrix as shown in Figure 1.5. [Qutubuddin et al. 2002; Gilman et al. 2000].

Conventionally, clays are not fully dispersed and form an agglomerated clay tactoid in the polymer matrix as shown in Figure 1.5 (a). In this case, clays are dispersed as a segregated and separated phase from the polymer matrix and the properties of composites are in the same range as in traditional microcomposites [Alexandre et al. 2000]. In this kind of system, mechanical properties of each individual layer in the clay particles are not fully realized because the interlayer bonding which is weak van der Waals force may act as fracture initiation site; high clay loading is required to achieve adequate improvement of the modulus, while strength and toughness of the polymer are reduced [Gao, 2004].

Beyond traditional microcomposites, two other types of structures which are called intercalated (Figure 1.5 (b)) and exfoliated (delaminated) (Figure 1.5 (c)) refer to the nanocomposites.

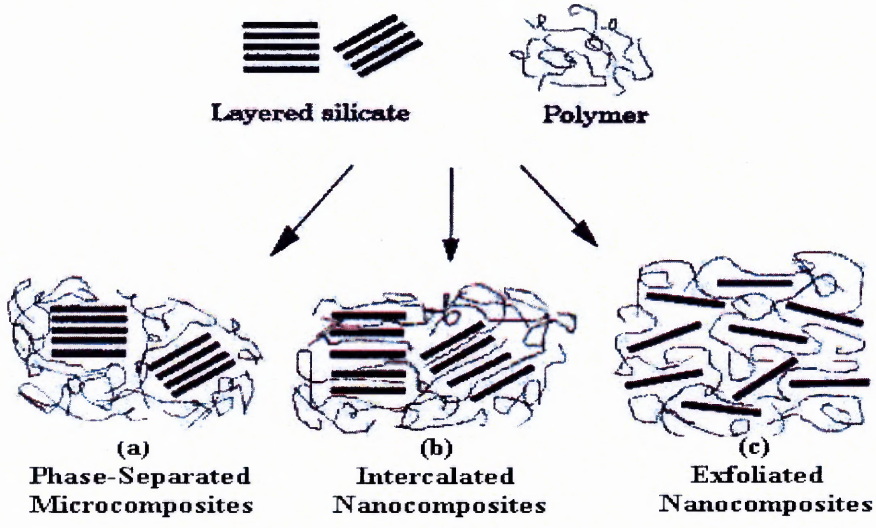

Figure 1.5 Schematic of different types of composites formed from the interaction of layered silicates and polymers: (a) phase-separated microcomposites, (b) intercalated nanocomposites, and (c) exfoliated nanocomposites
(Source: Alexandre et al. *Mater. Sci. Eng.* **2000**, 28, 1-63).

Intercalated structures are self assembled, well ordered multilayered structures where the extended single polymer chain or more than one chain are intercalated into the gallery space between parallel individual silicate layers separated by 2-3 nm. The intercalated nanocomposites typically have similar properties with those of ceramic materials [Kim 2006].

Exfoliated structures can be achieved as the individual silicate layers are completely dispersed in the polymer matrix, and are no longer close enough to interact with the adjacent layers' gallery cations. In this case, the interlayer spacing can be in the order of the radius of gyration of the polymer [Gilman et al. 2000]. The silicate layers in an exfoliated morphology may not be as well ordered as in an intercalated morphology. Hence, the silicate layers may be considered to be well dispersed in the organic polymer.

In these types of systems, individual clay particles which contain many layers can function effectively while the reinforcing factor is increasing. Therefore, a wide range of properties are significantly improved at low levels of filler loading. Both intercalated and exfoliated hybrid structures can also be found in the polymer matrix. Especially, smectite silicates which are having a layered structure (montmorillonite, hectorite and synthetic mica) disperse in the hybrid morphology [Gao, 2004].

1.4.2 Fabrication Technology of Nanocomposites

Since Blumstein (1961) intercalated vinyl group polymers into montmorillonite clay, several preparation methods of nanocomposites have been proposed.

In situ intercalative polymerization is inserting a precursor solution (monomer liquid or monomer solution) into the basal space of expanding layers, and then dispersing the clay layers into the matrix by polymerization. The polymerization can be initiated

either by heat or radiation, by diffusion of a suitable initiatior or by an organic initiator or catalyst fixed through cationic exchange inside the interlayer before the swelling step by the monomer. This method initially has been investigated by the Toyota research team which produced clay / nylon-6 nanocomposites [Okada et al. 1990, Usuki et al. 1996]. This method has been applied to a wide range of polymer systems because it is possible to achieve well exfoliated nanocomposites.

Lan et al. (1994) produced epoxy nanocomposite by *in situ* polymerization. In this case, montmorillonite was modified with alkylammonium chloride or bromide salts in H_2O/EtOH solution. Their study presented differences of montmorillonites modified at different reaction temperatures and times. X-ray diffraction patterns of the epoxy-clay composites showed exfoliated silicate clays which were expanded by the intercalated epoxy resin. Epoxy nanocomposites increased both the tensile strength and the modulus relative to pristine epoxy polymer.

Usuki et al. (1996) prepared polypropylene nanocomposites by *in situ* polymerization. Initially, organophilic clay (DSDM-Mt) was produced by a cationic reaction between MMT-Na^+ and the distearyldimethylammonium ion. A polyolefin oligomer with telechelic OH groups (Polyolefin diol, $C_{150\sim 200}$, Mitsubishi Chemical) was dissolved in toluene; the same quantity of DSDM-Mt was added to the solution. After evaporation of toluene, modified nanoclay (PODS-Mt) containing polyolefin diol in the basal space was produced. PODS-Mt and polypropylene were mixed in a mini-size mixer (Labo-Plastomill: Toyo Seiki), at 5 wt% of clay. TEM and XRD analyses proved the exfoliation of clays in the polypropylene matrix.

Wang et al. (2006) produced exfoliated hydrotalcite in a polymethyl methacrylate

(PMMA) matrix using *in situ* bulk polymerization of methyl methacrylate in the presence of 10-undecenoate intercalated layered double hydroxide. TEM picture showed the significant disordered nanoclay particles in the PMMA matrix. XRD results of composites did not include any diffraction peaks which would correspond to an exfoliated structure of the composite. Modified PMMA with tailored hydrotalcite showed better thermal stability and tensile modulus than pristine PMMA. The samples were analyzed by TGA, TEM, XRD, UV/visible transmission spectra and DSC.

The solution blending method applies to polymer solutions by swelling and dispersing the clays. Layered silicates can be easily dispersed in polymers dissolved in adequate solvents. The polymer is adsorbed onto the delaminated sheets and forms an ordered multilayer structure. The method has not been widely applied in industry because of the high cost of solvents and their safety issues. As a result, it has been focused especially on water based solutions and water soluble polymers, such as polyvinyl alcohol, polyethylene oxide etc.

Jeon et al. (1998) prepared high density polyethylene (HDPE) composites by solvent blending method. The montmorillonite was modified with dodecylamine to render the clay organophilic. 20 % of modified clay and 80% of HDPE were mixed in a co-solvent of xylene (80 wt%) and benzonitrile (20 wt%) at 100 ^{o}C for 30 minutes. The mixture was precipitated with large amounts of tetrahydrofuran (THF). XRD results showed that the basal space of modified MMT has been increased from 1.18 nm to 1.65 nm. Transmission Electron Microscope (TEM) characterization showed the layers to be aggregated in thin stacks which consist of a few individual layers.

In the melt processing method, the nanoclays are mixed with the polymer matrix

in the molten state. If the clay surfaces are compatible with the selected polymer, the polymer can increase the basal space and results in either intercalated or exfoliated nanocomposites; however, if the clay surfaces are incompatible with the selected polymer, macro-scale composites will be formed. Although the efficiency of melt processing may not be as high as that of *in situ* polymerization, this method has been applied by the polymer processing industry to produce nanocomposites based on traditional polymer processing techniques, such as extrusion and injection molding Therefore, the technology has been focused on speeding up the progress of the commercial production of clay/polymer nanocomposites. [Vaia et al. 1997, Gao 2004].

Liu et al. (1999) have produced nanocomposites based on commercial nylon-6 melt blended with an octadecylammonium-exchanged montmorillonite in a twin screw extruder at various loadings ranging from 1 to 18 wt %. At over 10 wt% filler content, an expanded basal space of the modified clay has been observed from 1.55 nm to 3.68 nm. At less than 10 wt% of filler content, diffraction peaks of XRD have not been detected which means a fully exfoliated morphology.

Because of its low polarity, polypropylene (PP) can not interact with commercial clays properly. Hence, direct intercalation of PP with modified layered silicates has not been carried out successfully by this method. Kato et al. (1997) first resolved this barrier by using either maleic anhydride (PP-MA) or hydroxyl groups (PP-OH) on the PP backbone. Under melt blending at 200 ^{o}C for 15 minutes, they examined the effects of polymer to clay ratio on the intercalation extent and showed increased interactions as the PP-MA fraction was increased. The basal space increased up to 7.22 nm for a PP-MA to clay ratio of 3:1.

To increase the thermal stability of the polyvinyl chloride (PVC), Lin et al. (2006) used tailored layered double hydroxides (LDH) which were MgAl-CO_3-LDH and MgZnAl-CO_3-LDH. Those tailored LDHs were synthesized by a specific process (Zhao 2002) and were blended with PVC for 10 minutes at 140 ^oC. Thermal stability tests proved that PVC containing MgAlZn-CO_3-LDH shows a higher thermal stability (stable at 180 ^oC for 187 minutes) than PVC without LDH (stable at 180 ^oC for 71 minutes).

In addition to these three major processing methods, other fabrication techniques have also been developed. These include solid intercalation, co-vulcanization, and the sol-gel method [Gao et al. 2001, Usuki et al. 2002, Musto et al. 2004].

1.5 Corrosion and Corrosion Inhibitors

Corrosion can be defined fundamentally as deterioration of properties of a material due to reactions with its environment such as water or oxygen. Corrosion can take place on many types of materials. However, in this research, corrosion of metal panels was examined as related to the improvement of the performance of anticorrosive coatings.

To prevent corrosion, two methods of inhibiting coatings are generally applied to metal substrates (Kooli et al 2003):

1. Corrosion inhibition by formation of organic or inorganic barriers: Created barrier coating on the metal surface restrains the corrosion by controlling the diffusion of the electrolyte, oxygen/protons and water.

2. Corrosion inhibition by corrosion inhibitors: Corrosion inhibitors can passivate the metal surface as a barrier. Passivating inhibitors undergo reduction at the active corrosion sites to form insoluble oxide that protect the further permeation of water, oxygen or electrolyte. The covered areas by corrosion inhibitors will prevent the permeability of electrolytes, water and oxygen thereby reducing the corrosion.

Organic corrosion inhibitor barriers usually are not sufficient to protect from corrosion by themselves because they contain micro-pores or areas of low cross linked density which provide a diffusion path for corrosive agents such as water, oxygen, and chloride ions to metal surface. Functional groups of organic corrosion inhibitors (carboxylates, amines, thiols, etc) form strong bonds to metal surfaces, but they also react with the functional groups (epoxies and isocyanates) that are commonly used to form thermoset coatings. Therefore, organic corrosion inhibitors can be trapped in the thermoset polymer by reaction with the coating resin and may not available for corrosion protection. Thus, there is a need to add corrosion inhibiting additives (e.g., clay) to enhance the corrosion protection of the substrate [Cook et al. 2006].

Cook et al. (2006) achieved better anticorrosive properties on aluminum /copper alloys by adding boehmite nanoparticles modified with organic corrosion inhibitors. The assumed mechanism was that bond between the boehmite nanoparticle surface and the functionality of the organic corrosion inhibitors could be cleaved by the hydroxyl anions formed by the cathodic reaction. Hence, the carriers would release the organic corrosion inhibitor as local pH increased. Improved anticorrosive performance by this method was confirmed by the salt fog corrosion test.

Buchheit et al. (2003) reported a pH-sensitive and corrosion protection coating by modifying hydrotalcite with decavanadate anions. In that study, anion exchanging hydrotalcite compounds dispersed as an additive in organic resins led to corrosion inhibition of an underlying aluminum alloy substrate. Released vanadate and Zn^{2+}, which are anodic and cathodic inhibitors, respectively, from the modified hydrotalcite played a key role of inhibiting corrosion of Al alloys. Ion exchange of hydrotalcite was confirmed by X-ray diffraction.

CHAPTER 2

EXPERIMENTAL SECTION

2.1 Materials

2.1.1 Ionic Liquids

The phosphonium based ionic liquids used in this study for clay modification include the following:

- trihexyltetradecylphosphonium tetrafluoroborate ([THTDP][BF_4])
- trihexyltetradecylphosphonium decanoate ([THTDP][DE])

Earlier data on clays modified with two imidazolium based ionic liquids were used for comparison [Kim et al. 2006 and Kim 2006]:

- 1-ethtyl-3-methylimidazolium bromide ([EMIM][Br])
- 1-hexyl-3-methylimidazolium chloride ([HXMIM][Cl])
- N-ethyl pyridimium tetrafluoroborate (Etpy][BF_4])

Trihexyltetradecylphosphonium tetrafluoroborate [THTDP][BF_4] and trihexyltetradecylphosphonium decanoate [THTDP][DE] were purchased from Sigma-Aldrich. Figures 2.1 and 2.2 show the chemical structures of the ionic liquids and Table 2.1 lists information on their properties.

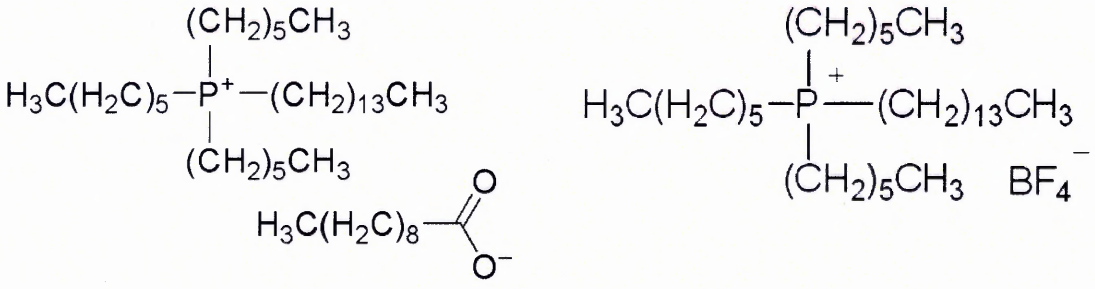

Figure 2.1 Structure of used ionic liquids: (left) trihexyltetradecylphosphonium decanoate [THTDP][DE], and (right) trihexyltetradecylphosphonium tetrafluoroborate [THTDP] [BF_4], [Sigma-Aldrich 2006].

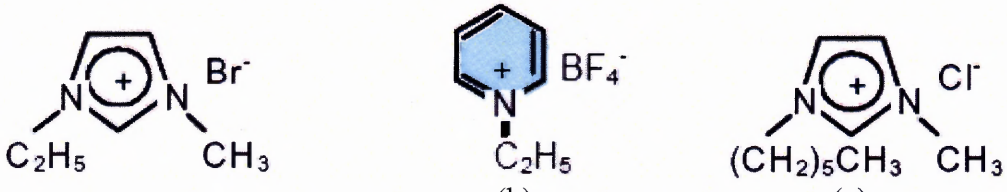

Figure 2.2 Structure of cited ionic liquids: (a) 1-ethyl-3methyl imidazolium bromide [EMIM][Br], (b) N-ethyl pyridimium tetrafluoroborate [Etpy][BF_4], (c) 1-hexyl-3methyl imidazolium chloride [HXMIM][Cl], [Kim 2006].

Table 2.1 Information on Ionic Liquids

Ionic liquid cation	anion	Molecular formula	M_w (g/mol)	Physical state at room temp.	Used in ion exchange
$THTDP^+$	$CH_3(CH_2)_8COO^-$	$C_{42}H_{87}O_2P$	655.13	Viscous liquid	cationic/ anionic
$THTDP^+$	BF_4^-	$C_{32}H_{68}BF_4P$	570.68	Viscous liquid	cationic/ anionic
$EMIM^+$	Br^-	$C_6H_{11}BrN_2$	191.07	Solid	cationic
$Etpy^+$	BF_4^-	$C_7H_{10}NBF_4$	194.80	Solid salt	cationic / anionic
$HXMIM^+$	Cl^-	$C_{10}H_{19}ClN_2$	202.72	Viscous liquid	cationic

(Source: Sigma-Aldrich MSDS 2006 and Kim 2006)

2.1.2 Halox® 520 (Liquid Organic Corrosion Inhibitor)

Halox® 520 (Hammond Group, USA) is a liquid organic corrosion inhibitor primarily designed for use in waterborne coatings systems. Reportedly, this additive not only inhibits corrosion but also promotes adhesion. The chemical structure of Halox® 520 is not fully disclosed by the manufacturer but is reported to contain a polymeric amine salt, 60 % active in ethanol. Physical properties and miscibility data are shown in Table 2.2 and 2.3.

Table 2.2 Physical Properties of Halox® 520

Physical Properties	
Appearance	Slightly yellow viscous liquid
Boiling Point	64 °C (1030 mbar, DSC)
Specific Gravity at 20 °C	0.93

(Source: Halox® 520 technical data 2003)

Table 2.3 Miscibility Data of Halox® 520

Miscibility (g/100g solution) at 20 °C	
Isopropanol	> 50 %
n-butanol	> 50 %
Diethylene glycol monomethyl ether	< 0.1%
Methyl-isobutyl-ketone	< 0.1%
Xylene	< 0.1%
Shellsol D40	< 0.1%
Water (pH 7)	< 0.1%

(Source: Halox® 520 technical data 2003.)

2.1.3 Nanoclays

2.1.3.1 Sodium Montmorillonite. Sodium montmorillonite (MMT-Na^+), used in this study was obtained from Southern Clay Products Inc. (CAS# 1318-93-0, trade name: Cloisite®-Na^+). MMT-Na^+ contains 4 - 9% moisture and sodium ions in the basal spacing without added organic modifiers. Its cationic exchange capacity (CEC) has been reported as 92.6 meq /100g clay. Molecular structure and other technical data are shown in Figures 2.3 and Table 2.4.

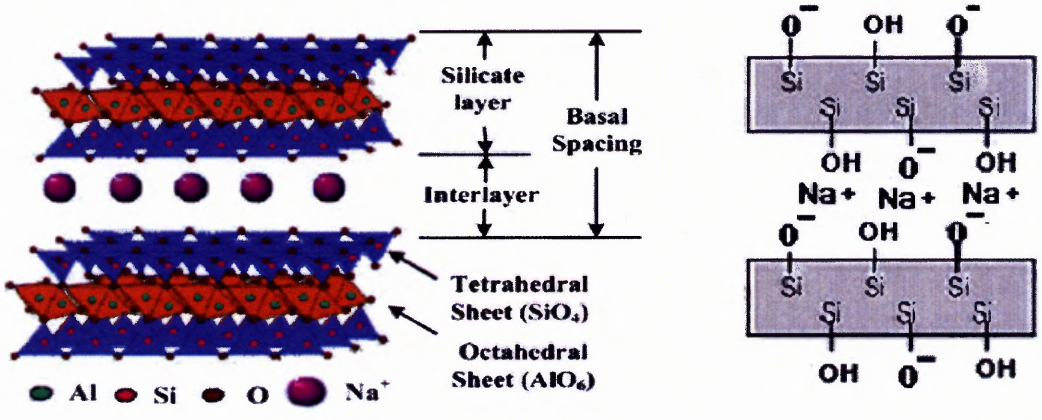

(a) (b)

Figure 2.3 (a) Schematic of molecular structure of MMT-Na^+, (b) Schematic side view of MMT-Na^+ between layers.
(Source: Mohanty, A., "The Future of Nanomaterials", Proc. Pira Intern. Conf., Feb. 22-24, Miami, Fl, 2005 and Kato et al."Polymer Clay Nanocomposites", Polymer Clay Nanocomposites ed. Pinnavaia T. J. and Beall G. W., John Wiley and Sons Ltd., New York, NY, 2000, pp97-109).

Table 2.4 Technical Data of Cloisite® Na^+ (MMT-Na^+)

X-ray result		
d_{001} = 11.7 Å		
Density		
Loose bulk (lbs/ft^3): 12.45	Packed bulk (lbs/ft^3): 20.95	Density (g/cc): 2.86
Typical Dry Particle size (Microns, by volume)		
< 10% : 2μm	< 50% : 6 μm	< 90% : 13 μm
Color		
Off white		

Source: Product Bulletin from Southern Clay Products Inc.

Cloisite® 15A, a commercial organoclay modified with quaternary ammonium salt (Sourthern Clay Products Inc., USA), was used for comparison to montmorillonite modified with ionic liquids. Technical data on Cloisite® 15A and the structure of the organic modifier are shown in Table 2.5 and Figure 2.4.

Table 2.5 Technical Data on Cloisite® 15A

X-ray result		
d_{001} = 31.5 Å		
Density		
Loose bulk (lbs/ft^3): 10.79	Packed bulk (lbs/ft^3): 18.64	Density (g/cc): 1.66
Typical Dry Particle size (Microns, by volume)		
< 10% : 2μm	< 50% : 6 μm	< 90% : 13 μm
Color		
Off white		

Source: Product bulletin from Southern Clay Products Inc.

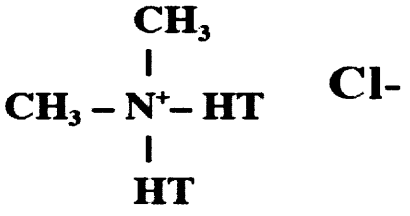

Organic Modifier:
2M2HT; Dimethyl, dehydrogenated tallow quaternary ammonium, where HT is hydrogenated tallow
(~ 65% C_{18}; ~30% C_{16}; ~5% C_{14})

Figure 2.4 Structure of organic modifier in Cloisite® 15A.
(Source: Technical Data of Southern Clay Products Inc.)

2.1.3.2 Hydrotalcite. A layered double hydroxide (LDH), which is also known as hydrotalcite (HT), is a synthetic aluminum magnesium hydroxyl carbonate. It was provided by Sasol, Germany (CAS # 1344-28-1, trade name: Pural MG 61 HT) and has a double layered metal hydroxide structure consisting of magnesium and aluminum hydroxide octahedral interconnected via the edges. The weight ratio of Al_2O_3 : MgO is reported as 39 : 61. The chemical formula of Pural MG 61 HT is $Mg_4Al_2(OH)_{20}CO_3nH_2O$, basal spacing is 0.77 nm (Sasol 2006) and the anionic exchange capacity was

theoretically calculated as 340 meq/100g (Kim 2006). A three-dimensional molecular structure is shown in Figure 2.6.

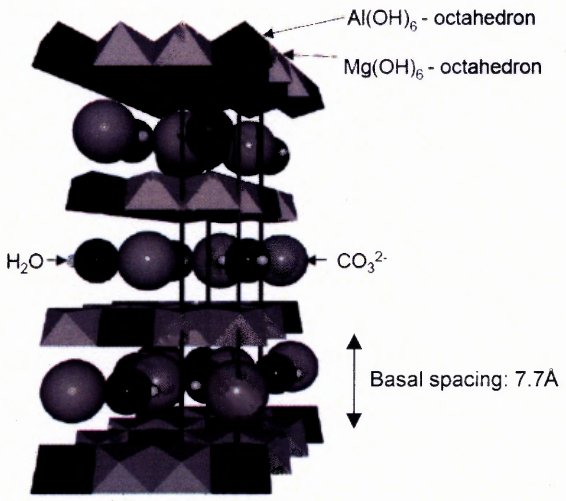

Figure 2.5 3D molecular structure of hydrotalcite.
(Source: Reijers et al. *Ind. Eng. Chem. Res.* **2006**, 45, 2522-2530).

2.1.4 Polymers

2.1.4.1 Polypropylene Polypropylene (PP) was obtained from ExxonMobile Chemical, USA (trade name: PP 4772). The reported melting point of PP is 165 ^{o}C and its glass transition temperature (Tg) is about -10 ^{o}C. Density of PP is 0.9 g/cm^3 and its MFI (Melt Flow Index) is 1.6 g/ 10 min. The chemical structure of polypropylene is shown in Figure 2.6 (a) [Kim 2006].

2.1.4.2 Modified Polypropylene. Because of the non-polar properties of polypropylene, the functionalized polypropylene with maleic anhydride (PP-g-MA) was used as a compatibilizer. Maleic anhydride grafted polypropylene was provided by Polyram, Israel (trade name: Bondyram 1001). 0.8 - 1.2 wt% of maleic anhydride is

grafted onto the polypropylene chain. The density of PP-g-MA was 0.91 g/cm^3, MFI is 100 g/ 10 min, and its melting temperature is 145-165 °C [Kim 2006].

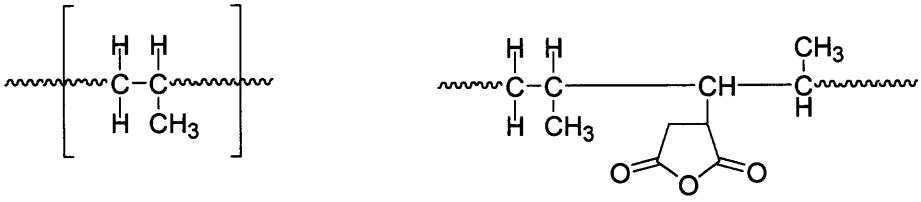

(a) **(b)**

Figure 2.6 Chemical structure of (a) polypropylene and **(b)** maleic anhydride grafted polypropylene.

2.1.4.3 Polycrylic® paint. Polycrylic® is a water based vinyl acrylate protective finish which is produced by Minwax, USA. According to manufacturer's data Polycrylic® has specific gravity of 1.02 – 1.03, 71% volatile content (water and a minor amount of organic solvent) and a measured pH of 8.38 at 37 °C. The calculated density for the solid polymer was 1.036 g/cc. Because of its fast drying properties and poor corrosion protection, it was considered as suitable for accelerated corrosion tests of steel panels.

2.2 Clay Modification through Ion Exchange

2.2.1 Cationic Exchange

Both phosphonium based ionic liquids were evaluated as organic modifiers for MMT-Na^+. The ion exchange reactions were carried out at different times and temperatures.

Initially, a control experiment (MMT-1) was carried out without ionic liquid. For the cationic exchange reactions, [THTDP][BF_4] and [THTDP][DE] were added at 2X the stoichiometric amounts of the cationic exchange capacity (CEC) (3.16 g and 3.65 g

respectively in 250 ml solution) of MMT-Na^+. The two ionic liquids were dissolved in ethanol (200 ml) and deionized water (50 ml) solution by vigorous stirring for 10 minutes at room temperature. MMT-Na^+ (3 g) was then added to the solution. Cationic exchange reactions were performed under three different conditions under reflux. Specific experimental conditions and abbreviations are presented in Table 2.6.

Table 2.6 List of Cationic Exchange Reactions and Abbreviations

Solution	Abbreviations of MMTs	Host clay	Organic modifiers	Temp (under reflux)	Time
EtOH and Deionized water (200ml : 50ml)	MMT-1	MMT-Na^+	N/A	60 °C	5hrs
	MMT-2	MMT-Na^+	[THTDP][DE]	60 °C	5hrs
	MMT-3	MMT-Na^+	[THTDP][BF_4]	60 °C	5hrs
	MMT-4	MMT-Na^+	[THTDP][DE]	80 °C	5hrs
	MMT-5	MMT-Na^+	[THTDP][BF_4]	80 °C	5hrs
	MMT-6	MMT-Na^+	[THTDP][DE]	60 °C	24hrs
	MMT-7	MMT-Na^+	[THTDP][BF_4]	60 °C	24hrs
	MMT-8	MMT-Na^+	Halox® 520	60 °C	24hrs

The modified MMTs were collected by vacuum filtration (Genuine Whatman filter paper, 7 cm diameter, 1.6 μm pore size). The collected modified MMTs were washed many times in the funnel with EtOH / H_2O (EtOH 80 %, H_2O 20 %) solution and then washed three times again with vigorous stirring in a 500ml beaker to remove residual anions. MMTs were collected by vacuum filtration again after each washing and the finally filltered MMTs were dried at room temperature for 24 hours and then at 90°C

for 24 hours under vacuum. The final products were ground with a mortar and pestle and dried at 90°C for 24 hours under vacuum once again.

In the case of modification of MMT-Na^+ with Halox® 520, 250ml of EtOH was used as a solvent with a slight amount of de-ionized water. Due to limited information on Halox® 520, an assumption was made that it had the same cationic exchange capacity as [THTDP][DE]. 6 g of Halox® 520 were added to the ethanol solution at room temperature and then the mixture was stirred for 30 minutes. MMT-Na^+ (3g) was then added to mixture. Specific reaction conditions are shown at Table 2.6. The subsequent steps were the same as for the ionic liquids exchange.

2.2.2 Anionic Exchange

Hydrotalcite was only modified with [THTDP][DE] in this study. In previous research [Kim 2006], it was realized that small anions intercalated into the basal spacing of hydrotalcite, would not increase the interspacing distance, significantly. The anion of [THTDP][DE] is one of the largest anions among the available ionic liquids and, thus, it was expected to increase the basal spacing significantly. The condition for the exchange reaction, filtration, and drying steps were the same as for the previous cationic exchange reactions.

Calcined hydrotalcite, after removing CO_3^{2-} and H_2O by heating at 480 °C for 5 hours in the furnace, was also used. The calcined hydrotalcite was kept in the desiccator prior to use in order to prevent hydration or absorption of carbon dioxide. Hydrotalcite modification was based on the assumption that the empty basal space of the calcined

hydrotalcite may be regenerated by ion exchange with the ionic liquid. Specific abbreviations and experimental conditions are shown in Table 2.7.

Table 2.7 List of Anionic Exchange Reactions and Abbreviations

Solution	Abbreviations of HTs	Host clay	Organic modifiers	Temp (under reflux)	Time
EtOH and Deionized water (200ml : 50ml)	HT-1	Hydrotalcite	N/A	60 °C	5hrs
	HT-2	Hydrotalcite	[THTDP][DE]	60 °C	5hrs
	HT-3	Hydrotalcite	[THTDP][DE]	60 °C	24hrs
	CHT-1	Calcined Hydrotalcite	N/A	-	-
	CHT-2	Calcined Hydrotalcite	[THTDP][DE]	60 °C	24hrs

2.3 Sample Preparation

2.3.1 Polypropylene Nanocomposites

Polypropylene nanocomposites (PNCs) were prepared in a Brabender mixer (PL2000, C.W. Brabender; maximum capacity: 60 cm^3). The weight of the entire mixture was 42 g. This value was chosen to minimize the free space in the chamber and maximize the efficiency of mixing.

The PP and PP-g-MA mixture was loaded into the chamber set at 180 °C and a rotation speed of 50 rpm. When the torque of the PP/PP-g-MA mixture stabilized (usually 4 or 5 minutes later), the calculated amount of clay was added into the chamber. The mixture was compounded for another 15 minutes. The composites were then compression molded in a PHI press for 2 minutes at 180 °C to form test discs (diameter: 4 cm, thickness: 1.5 mm). The list of the experiments is shown in Table 2.8.

Table 2.8 List of Compounding Experiments

Abbreviation	Base Polymer	Compatibilizer (Comp.)	Clay types	Weight Ratio Polymer/comp./Clay
PNC-1	PP	PP-g-MA	N/A	85/15
PNC-2	PP	PP-g-MA	MMT-1	85/10/5
PNC-3	PP	PP-g-MA	MMT-6	85/10/5
PNC-4	PP	PP-g-MA	MMT-7	85/10/5
PHT-1	PP	PP-g-MA	N/A	85/15
PHT-2	PP	PP-g-MA	HT-1	85/10/5
PHT-3	PP	PP-g-MA	HT-3	85/10/5
PCHT	PP	PP-g-MA	CHT	85/10/5
PNC-15A	PP	PP-g-MA	Cloisite® 15A	85/10/5

2.3.2 Preparation of Modified Paint Film

Polycrylic® was used as the base paint; base paint films containing the commercial inhibitor, nanoclays, and nanoclay modified with the commercial inhibitor were prepared for comparison. Neat Polycrylic® and modified paints were applied on steel panels by standard drawdown techniques at 4 mil thickness. Coated panels were immersed into simulated sea water (1M NaCl solutions) for 3 days. The panels were then visually compared for rust formation. Specific compositions are listed in Table 2.9.

Table 2.9 List of Paint Coated Panels

Abbreviation	Substrate	Paint	Filler (5wt%)
Coat-1	Fe Panel	Polycrylic®	MMT-1
Coat-2	Fe Panel	Polycrylic®	Halox 520
Coat-3	Fe Panel	Polycrylic®	MMT-8

2.4 Charaterization

Thermogravimetric Analysis (TGA): In order to compare the thermal stability of uncoated and modified clays, TGA (TA instruments' QA 50 thermogravimetric analyzer) was carried out using a ramp from room temperature to 500 °C, at a heating rate of 15 °C / min in nitrogen atmosphere.

Fourier Transform Infrared Spectroscopy (FT-IR): FT-IR was used to confirm that the ionic liquids were intercalated in the basal spacing of the clays. The range of FT-IR wavenumbers was between 400 - 4000 cm^{-1} and the sample was scanned 20 times. Small amounts of clays and modified clay (1 wt%) were mixed with fully dried potassium bromide (KBr). A thin pellet was then prepared at 12000 lb/cm^2 by pressing in a die (International Crystal Laboratory). In the case of ILs, due to their liquid like properties at room temperature, horizontal attenuated total reflection (HATR) method was used.

Wide Angle X-ray Diffraction (WXRD): Philips PW3040 diffractometer (Cu Kα radiation λ=1.5406 Å, generator voltage = 45 kV, current = 40 μA) was used to evaluate increase in the basal spacing of the nanoclays. 2θ range was scanned from 2° - 20° for every sample. The basal spacing of clays was calculated by the Bragg's law of diffraction (Equation 2.1).

$$2d = n\lambda/\sin\theta \quad (2.1)$$

Where, n is an integer 1, in our case, λ is the wavelength of the incident X-ray beam in Å, and θ is the angle of incidence in degrees.

Scanning Electron Microscopy (SEM): Cross-sections of the nanocomposites which were prepared with uncoated and modified clays were observed by LEO 1530VP Emission Scanning Electron Microscope (LEO Gemini column) with an electron beam in the spectral range of 5-7 KeV working voltages.

Transmission Electron Microscopy (TEM): TEM images of nanocomposites were taken at Inha University, South Korea with a Philips CM200 Electron microscope. A small piece of each composite was mixed with epoxy resin contains the curing agents listed in Table 2.10 in the embedding capsule (Ted Pella). The mixtures were cured at 60°C for 24 hours under vacuum. 50 nm thick layers were used for observation.

Table 2.10 Composition of Epoxy Embedding Materials

1.	Nadic Methyl Anhydride (NMA)	1.025 g
2.	Glycerol Polyglycidyl Ether (Eponate 12 resin)	1.57 g
3.	Dodecenyl Succinic Anhydride 2X distilled (DDSA)	0.465 g
4.	2,4,6-tris(dimethylaminomethyl)phenol (DMP-30)	0.04 g

CHAPTER 3

RESULTS AND DISCUSSION

This section will provide the results from experiments carried out to elucidate the effects of different ionic liquids and Halox® 520 for sodium-montmorillonite ($MMT\text{-}Na^+$), hydrotalcite containing carbonate ions (HT-61), and calcined hydrotalcite (CHT) on the properties of nanoclays.

3.1 Sodium Montmorillonite Modification by Cationic Exchange

Modification of $MMT\text{-}Na^+$ by cationic exchange with ionic liquids (ILs) was carried out at three different conditions (60 °C for 5 hours, 60 °C for 24 hours and 80 °C for 5 hours). Modified $MMT\text{-}Na^+$ with the organic corrosion inhibitor was also prepared under similar conditions. A list of abbreviations and cationic exchange conditions are shown in Table 2.6.

Unlike ion exchange in water based solutions of low molecular weight ILs (Kim 2006), cationic exchange of the higher molecular weight ILs in 80% EtOH and 20% de-ionized water solution did not create any difficulties of filtration or grinding. Each filtration took less than 10 minutes, and the clay cakes were easily detached from the filter paper.

3.1.1 Thermogravimetric Anaysis

The TGA results of MMTs modified with different ILs by cationic exchange were compared with those of the pristine MMT (MMT-1). The weight percentage of intercalated ionic liquids was evaluated. TGA results of the cationic modification of MMT show higher amount of IL retained at 60 °C and 24 hours than other conditions such as 60 °C/5 hr, 80 °C/5 hr. As a result all analytical data reported below are based on these conditions.

The thermal stability of the ionic liquids is shown in Figure 3.1. The [THTDP][BF_4] is more thermally stable than [THTDP][DE]. Since both ionic liquids have the same cation, the different anion is responsible for the different thermal stabilities.

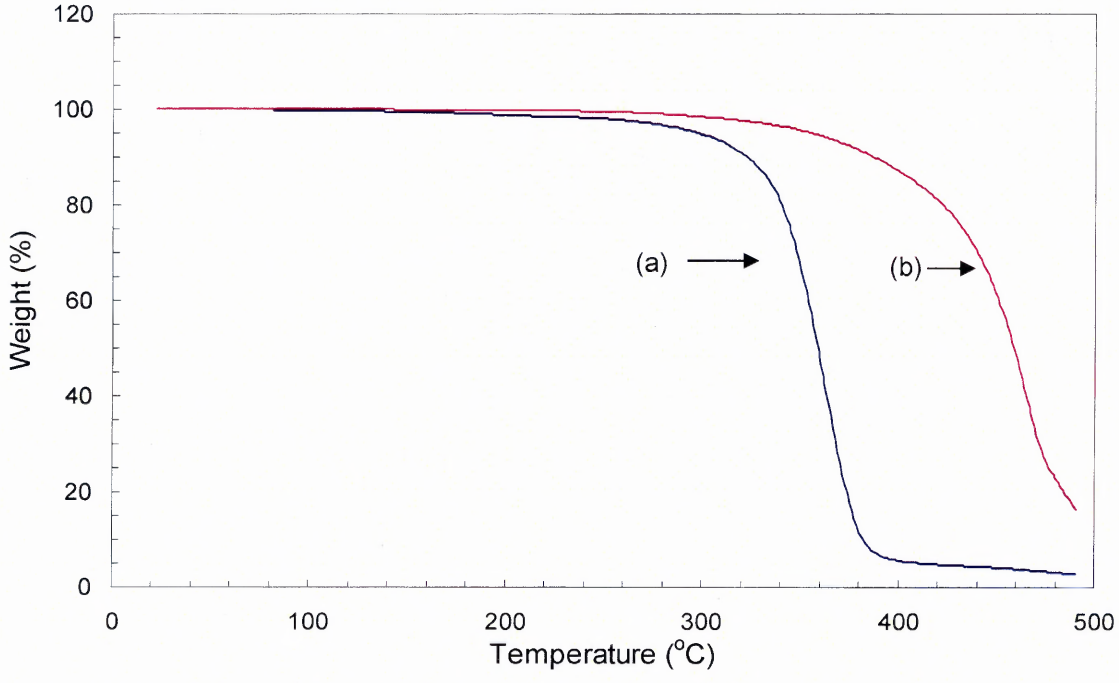

Figure 3.1 TGA results of (a) [THTDP][DE] and (b) [THTDP][BF_4].

Both phosphonium based ionic liquids (Figure 3.1) have higher thermal stability than imidazolium based ionic liquids (Figure 3.2 (I) and (II)) previously used for the cationic modification of the nanoclay. Hence, it was expected that the modification of MMT with phosphonium based ionic liquids would produce more thermally stable materials than MMTs modified with the imidazolium based ionic liquids. However, TGA results of pyridinium based IL (Figure 3.2 (III)) shows similar thermal stability as for [THTDP][BF_4]. Since both ionic liquids have the same anion (BF_4^-), it is confirmed that thermal stabilities of the ILs depend to a large extent on the type of anion.

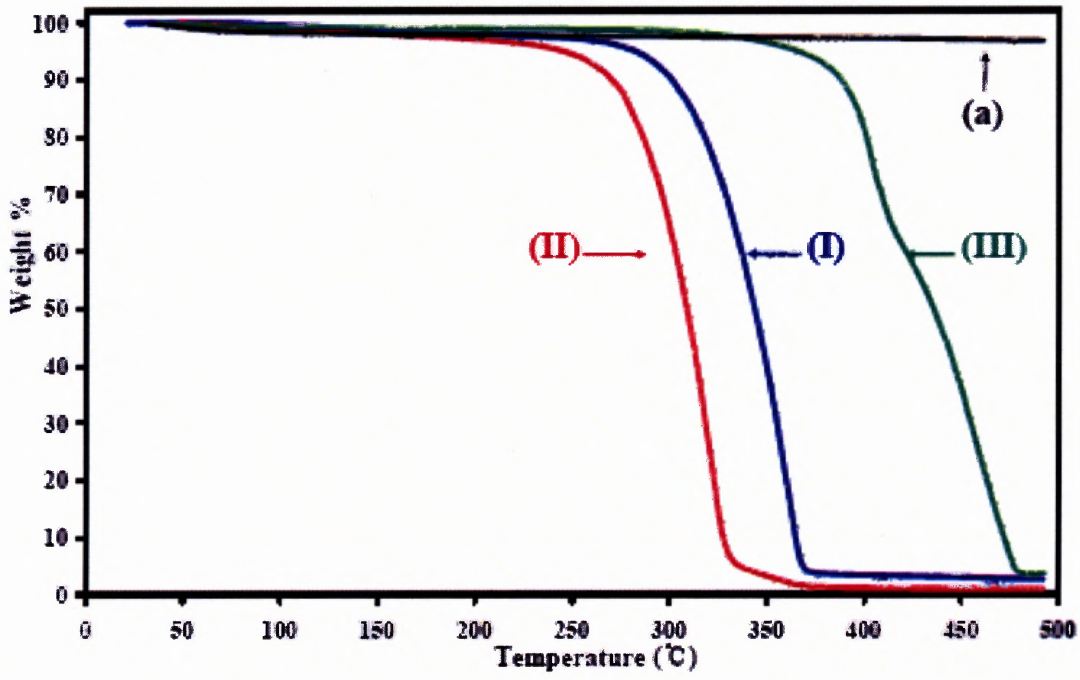

Figure 3.2 TGA results of (a) unmodified MMT, (I) [EMIM][Br], (II) [HXMIM][Cl], (III) [Etpy][BF_4].
(Source: Kim et al. *Microporous and Mesoporous Mater.* **2006,** 96, 29-35.)

The thermal stabilities of MMT-6 and MMT-7 are shown in Figure 3.3 and Figure 3.4, respectively. These modified clays have significantly higher thermal stability than commercial nanoclays such as Cloisite® 15A and Cloisite® 30 (Kim et al. 2006)

(Appendix A). Comparing with MMT-1, MMT-6 (nanoclay modified with [THTDP][DE]) lost 10.3 wt% at 500 °C; MMT-7 (nanoclay modified with [THTDP][BF_4]) lost 10.9 wt% at 500 °C. The similarity in the percent weight loss at 500 °C is due to the presence of the same cations from both ionic liquids and the removal of the anions that are contributing to the observed different thermal stability (Figure 3.1). The thermal stability of MMT-8 modified with the organic corrosion inhibitor (Halox® 520) is shown in Figure 3.5. The weight loss differences between MMT-1 and MMT-8 is 5.81 wt% at 500 °C.

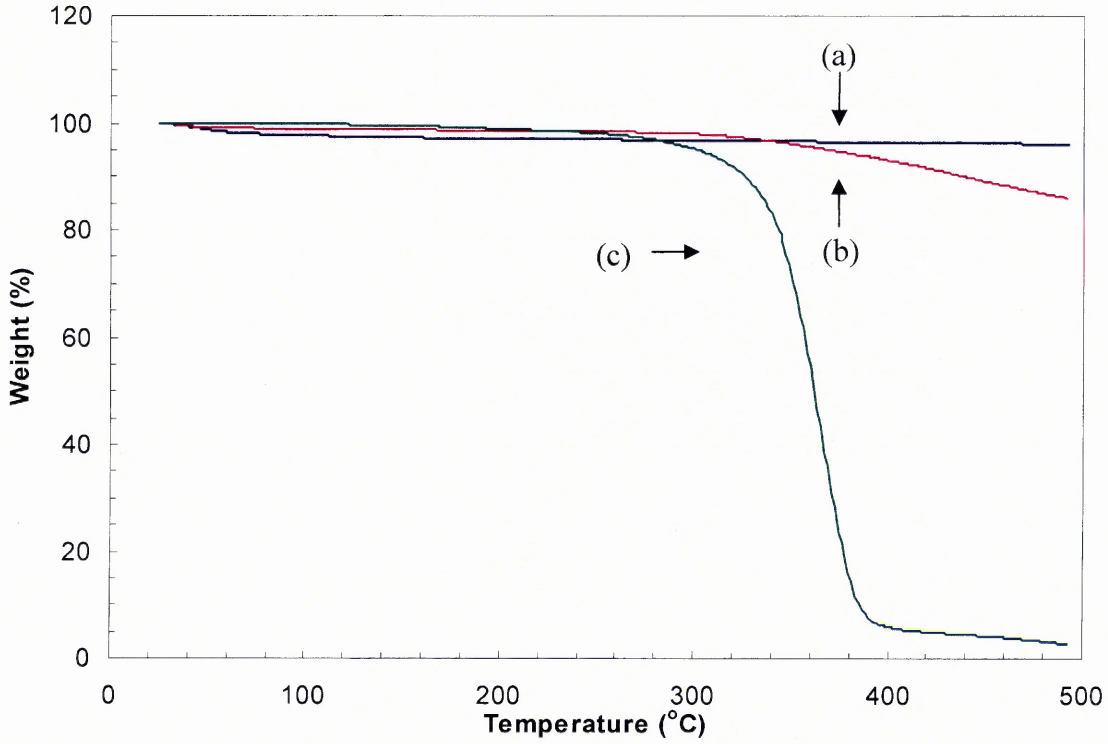

Figure 3.3 TGA results of (a)MMT-1, (b)MMT-6, and (c)[THTDP][DE].

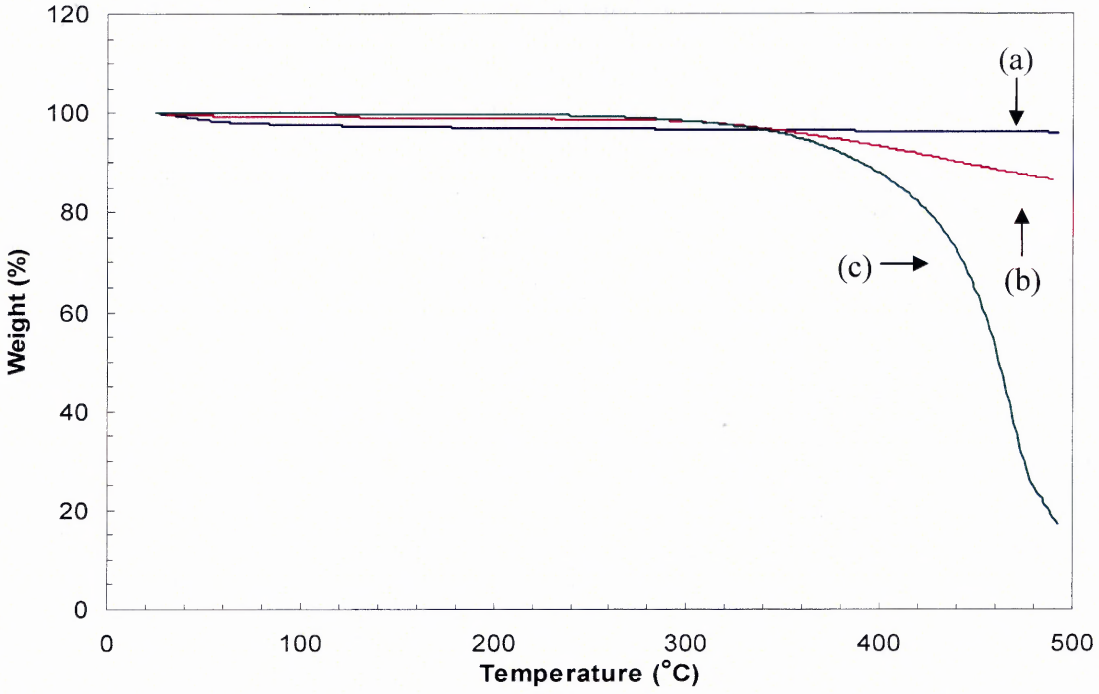

Figure 3.4 TGA results of (a) MMT-1, (b) MMT-7, and (c) [THTDP][BF_4].

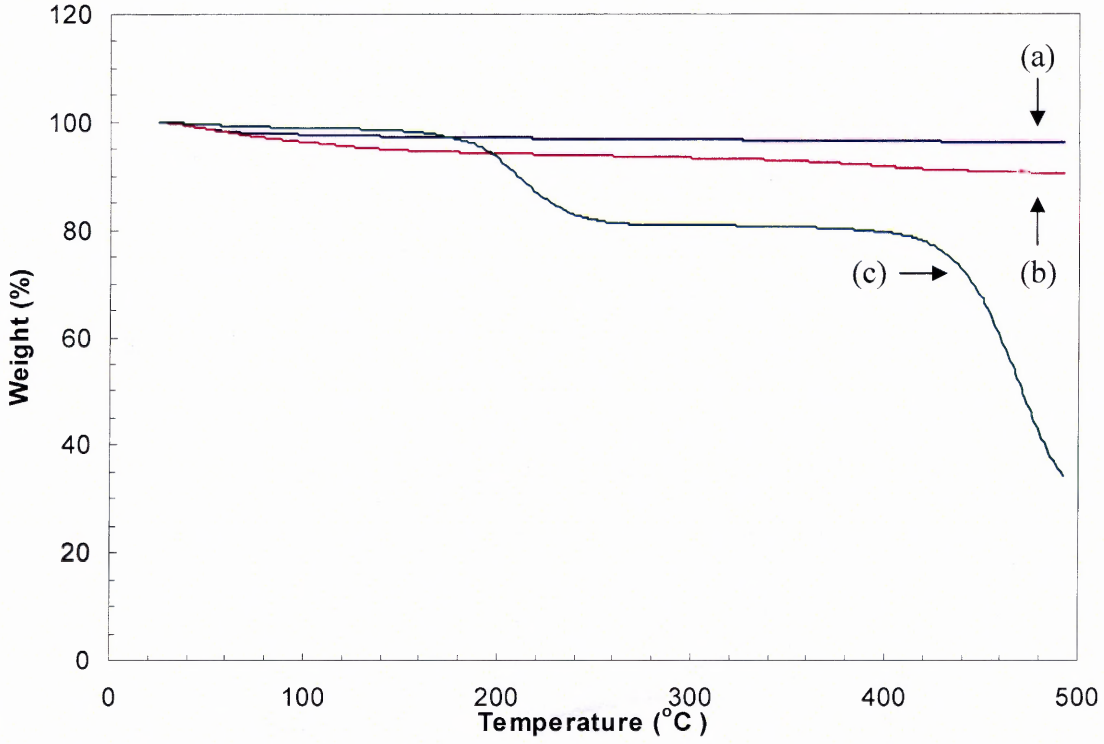

Figure 3.5 TGA results of (a) MMT-1, (b) MMT-8, and (c) Halox® 520.

3.1.2 Fourier Transform Infrared Spectroscopy

The FT-IR analysis was mainly carried out for comparing the difference between unmodified MMT and MMT modified with both the phosphonium based ILs.

The spectrum of sodium montmorillonite (MMT-1) is shown at Figure 3.6 (a); the peaks at 1044 cm^{-1} and 620 cm^{-1} represent the silicon-oxygen and aluminum-oxygen bonds, respectively. A band between 470 cm^{-1} and 530 cm^{-1} represents the magnesium-oxygen but the strong peak at 1650 cm^{-1} and broad band at 3440 cm^{-1} have been assigned to the bending and stretching modes of absorbed water (Kim 2006).

The spectrum of [THTDP][DE] is shown in Figure 3.6 (c). Carbon-carbon bending and stretching are observed at 500 cm^{-1} and in the region between 800 cm^{-1} and 1200 cm^{-1}, respectively. Carbon-hydrogen stretching peaks are shown in the range of 2840 - 3000 cm^{-1} with the band between 2872 cm^{-1} - 2962 cm^{-1} representing methylene groups (asymmetric stretching 2853 cm^{-1}, symmetric stretching 2926 cm^{-1}). The peaks for carbon-hydrogen bending are detected at 1375 cm^{-1}, 1465 cm^{-1}, 720 cm^{-1}, and in the 1350 cm^{-1} – 1150 cm^{-1} region. Peaks assigned to phosponium based organic groups (1300-1275 cm^{-1}) are very weak (Figure 3.6 (c)).

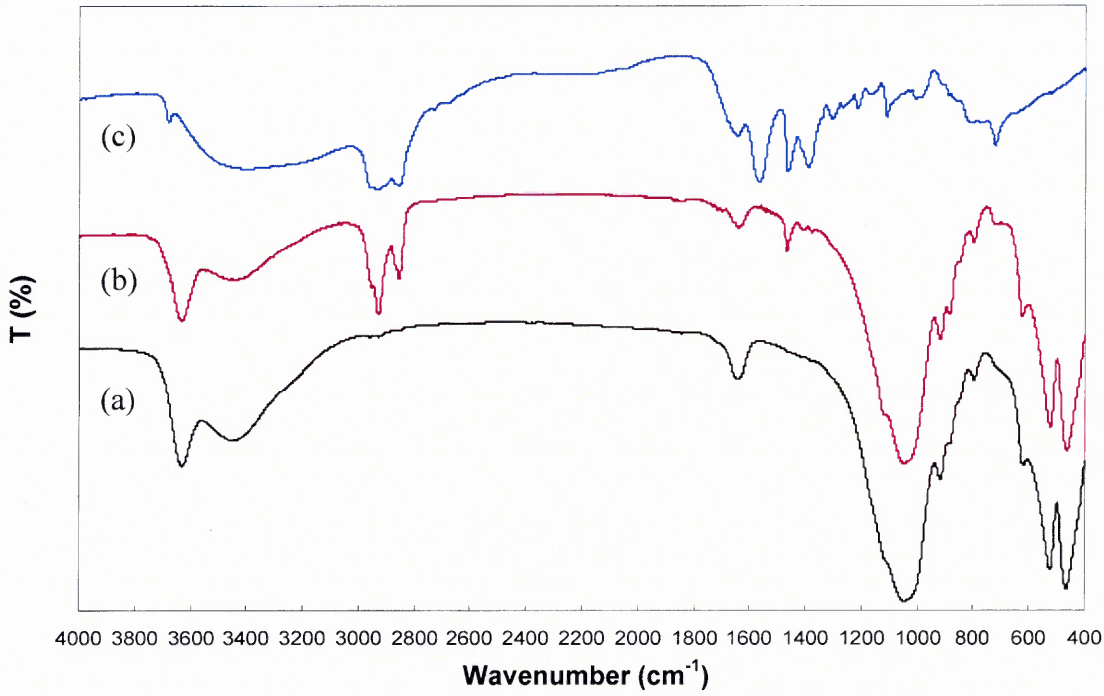

Figure 3.6 FTIR spectra of (a) MMT-1, (b) MMT-6, and (c) [THTDP][DE].

The presence of the peaks of the peaks in the range of 2840 - 3000 cm^{-1} and at 1450 cm^{-1} of MMT-6 (Figure 3.6 (b)) is an indication of exchanged [$THTDP^{+}$] cation in the basal spacing of the nanoclay. This is evident from comparison of the spectra of MMT-1 and MMT-6 with [THTDP][DE]. It is believed that MMT-6 may not contain the residual anion since the assigned to COO^{-} stretching peaks (asymmetric: 1592 cm^{-1} and symmetric: 1412 cm^{-1}) are not apparent (Figure 3.6 (b)).

The spectrum of nanoclay modified by cationic exchange with [THTDP][BF_4] (Figure 3.7(b)) has a close resemblance with the spectrum of MMT-6. Since the ILs have different anions, these spectra confirm that no residual anions remained after the cationic exchange reactions.

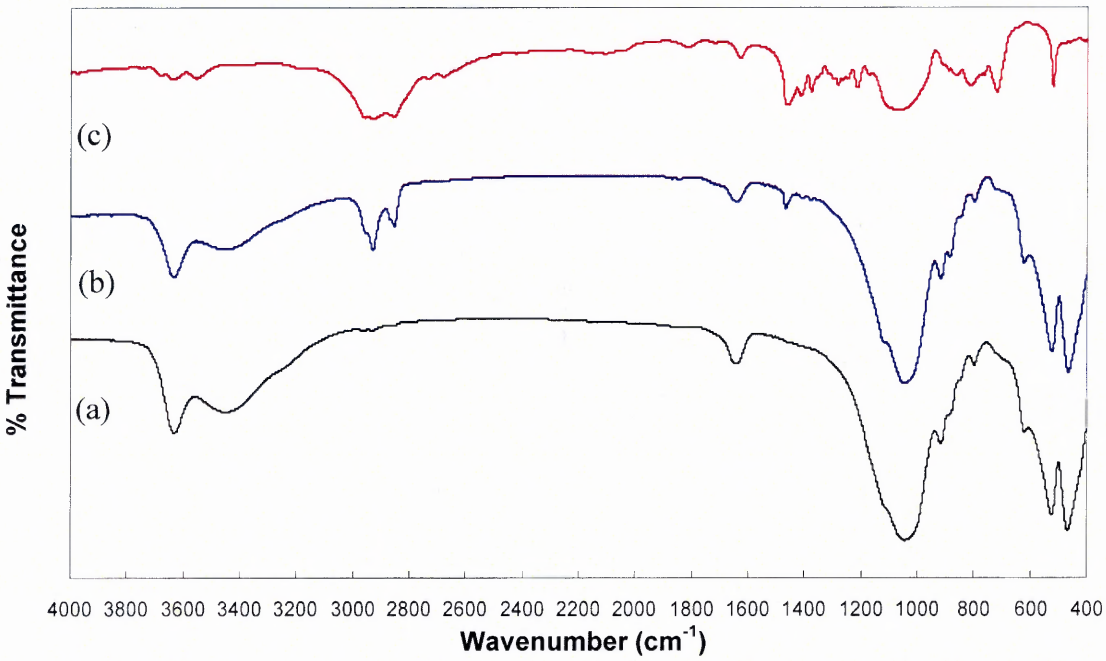

Figure 3.7 FTIR spectra of (a) MMT-1, (b) MMT-7, and (c) [THTDP][BF_4].

According to the manufacturer's data, Halox® 520 is comprised of polyamine and fatty acid in the form of a salt. Figure 3.8 shows the spectrum of the Halox® 520 after removal of solvent and Figure 3.9 shows the spectra of MMT-1 and MMT-8. By comparison of spectra in Figure 3.8 and Figure 3.9 indicate after modification MMT-8 contains certain peaks that originally appeared in the spectrum of Halox® 520 as for example at 2840 - 3000 cm^{-1} and 1375 - 1450 cm^{-1}. This is an indication of possible anchoring of the cation of Halox® 520 to the MMT-1. In the absence of additional information on the structure of Halox® 520 further analysis of the spectra is not possible.

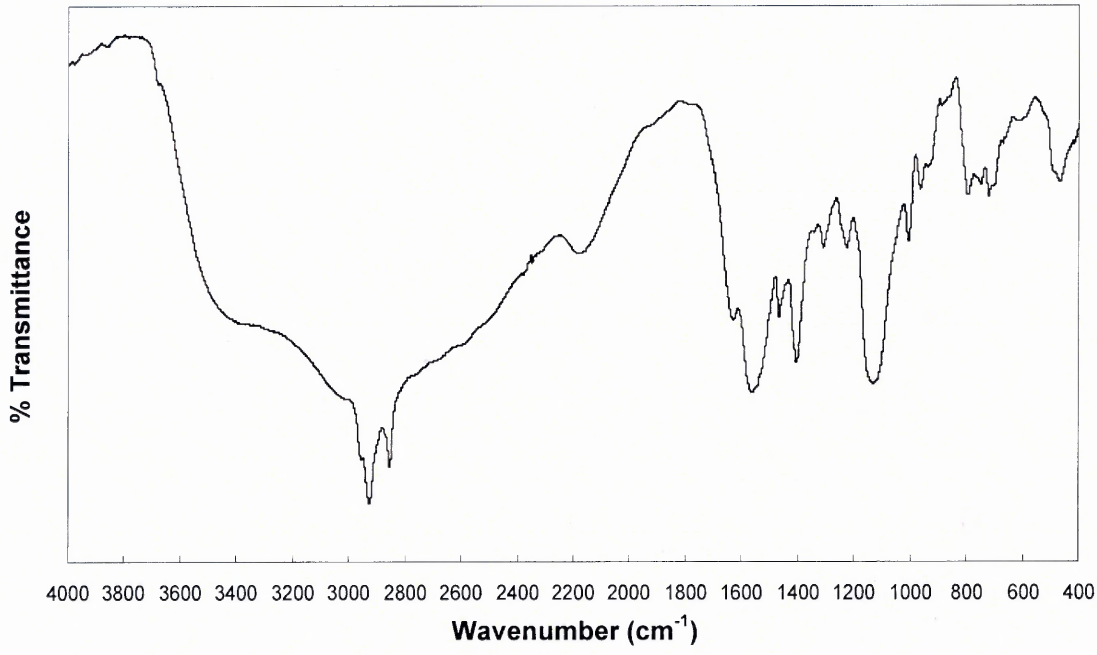

Figure 3.8 FTIR spectrum of Halox® 520.

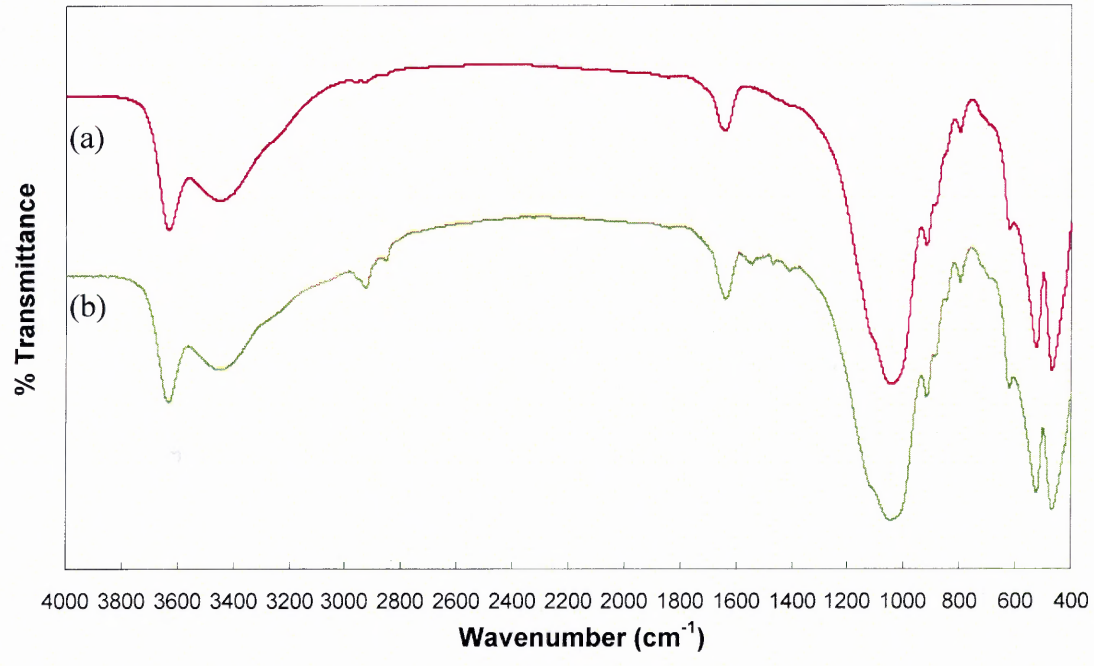

Figure 3.9 FTIR spectra of (a) MMT-1 and (b) MMT-8.

3.1.3 Wide Angle X-Ray Diffraction

The WXRD analysis was performed in order to observe the basal spacing change between layers after exchanging sodium ions with the cations of the ionic liquids or the cations of the organic corrosion inhibitor.

A comparison of the WXRD results for MMT-1 and MMT6 are shown in Figure 3.10. The peak for unmodified MMT-1 is observed at 2θ = 8.97° and this corresponds to a basal spacing of 0.94 nm. The modified nanoclay, MMT-6, has a basal spacing of 1.82 nm at 2θ = 4.85° which is twice the spacing of MMT-1. The increased basal spacing of MMT-6 indicates that the larger cation from the [THTPD][DE] increases the interspacing by replacing the sodium ions of MMT. Therefore, it appears that the cationic exchange of nanoclay has been successively carried out.

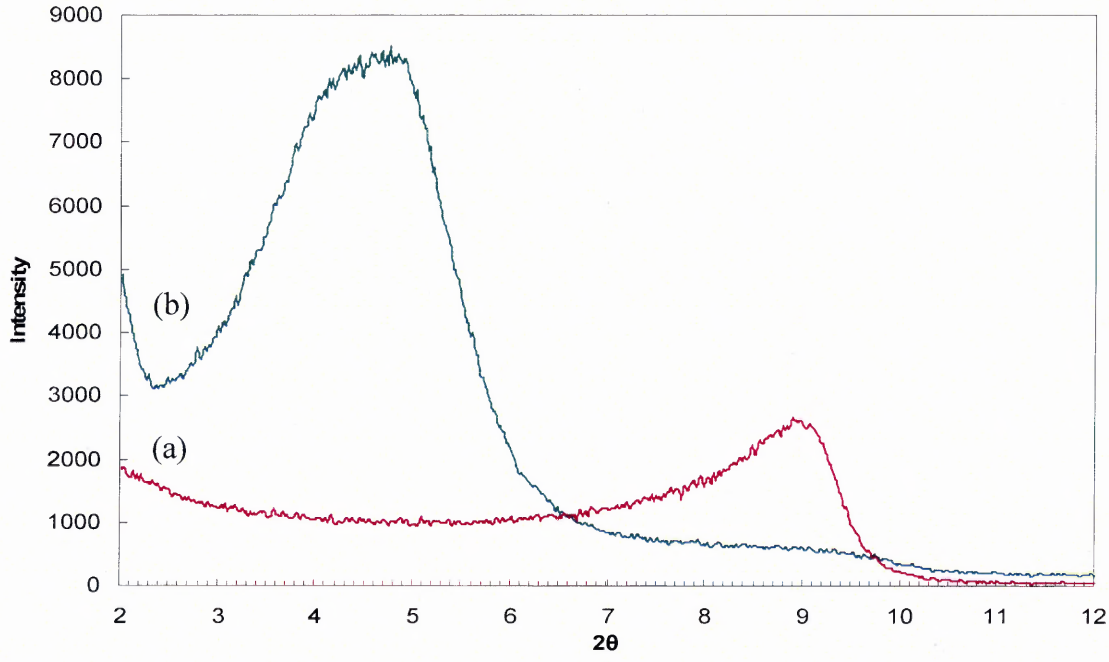

Figure 3. 10 WXRD results of (a) MMT-1 (2θ=8.97°: 0.94 nm) and (b) MMT-6 (2θ=4.85° : 1.82nm).

Figure 3.11 shows the shifting to a 1.87 nm basal spacing for MMT-7 from the 0.94 nm basal spacing of MMT-1 as a result of the cationic modification with [THTDP][BF_4]. The similar basal spacings of MMT-6 and MMT-7 are due to the same cations present in both ionic liquids.

Compared to nanoclays modified with lower molecular weight cations, the higher molecular weight cations in our ILs increase interspacing to a larger extent. The basal spacings of clays modified with different cations are compared in Table 3.1[Kim 2006 and Southern Clay Products Inc.].

In Figure 3.12, the WXRD spectrum of MMT modified with the organic corrosion inhibitor is shown along with the spectrum of the unmodified MMT. The inter spacing has been increased from 0.94nm to 1.82 nm presumably by the cation of the organic corrosion inhibitor

Table 3.1 Basal Spacings of Unmodified and IL-Modified Clays

Nanoclay	Organic modifier	Basal spacing
MMT	None	0.94nm
	[THTDP][DE]	1.82nm
	[THTDP][BF_4]	1.87nm
	[EMIM][Br]	1.40nm
	[HXMIM][Cl]	1.26nm
	2M2HT	3.13nm

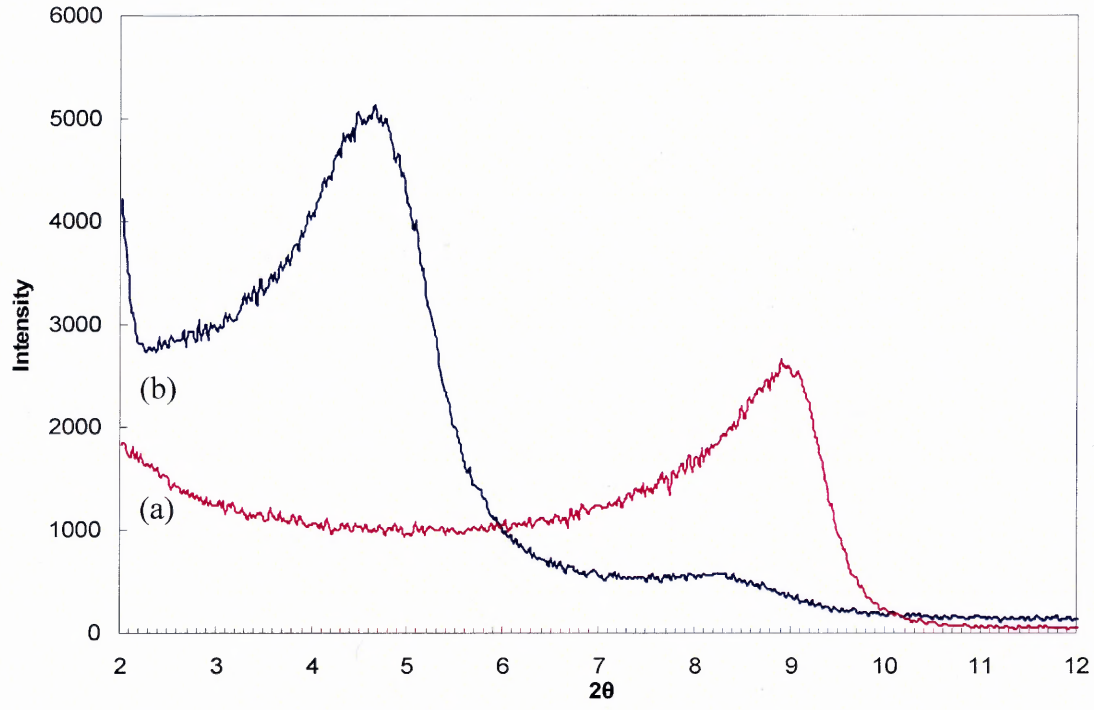

Figure 3. 11 WXRD results of (a) MMT-1(2θ=8.97°: 0.94 nm) and (b) MMT-7 (2θ= 4.71°: 1.87 nm).

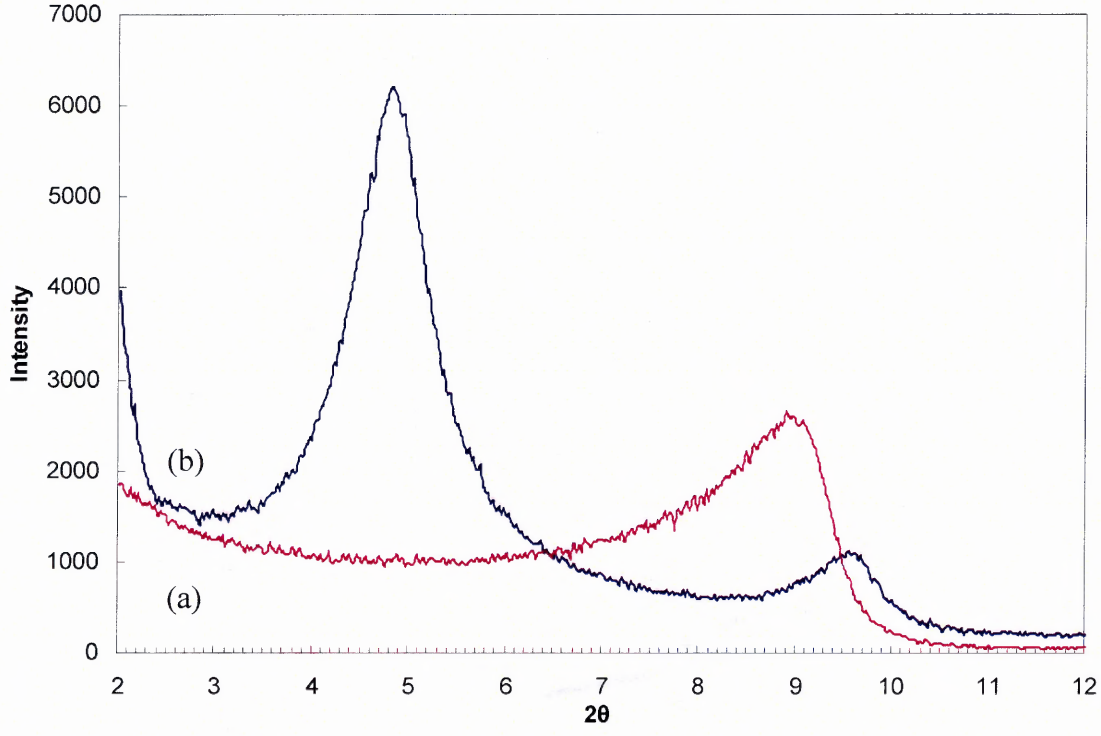

Figure 3.12 WXRD results of (a) MMT-1(2θ=8.97°: 0.94 nm) and (b) MMT- 8 (2θ = 4.85° : 1.82 nm).

3.1.4 Accelerated Corrosion Test

Simulated sea water conditions were carried out by using a 1 M NaCl solution as a medium for accelerated corrosion. This test was performed to find the differences among anti-corrosive protective coatings applied on steel panels containing clays and corrosion inhibitors in a commercial paint. During the immersion test, red rust was attached on the coatings. This red rust was presumably created by corrosion in the other side of the steel panel where the coatings were not applied. Therefore, visual comparison was done after stripping the red rust from the coated surfaces and detaching the coating from the panels.

Figure 3.13 Immersion test results in 1M NaCl solution for 3 days (a) Coat-1, (b) Coat-2, and (c) Coat-3.

As shown in Figure 3.13, Coat-3 (MMT-8) contains both inhibitor and clay indicates the best protection after a three days immersion test as shown by absence of visual corrosion signs. By contrast, Figure 3.13(b) (5wt% of Halox® 520) shows many tiny black spots which are suspected to be signs of corrosion. Black spots on Coat-1(5

wt% of MMT-1) are also apparent. Although specific mechanisms for the different behavior of coatings are not yet clear, it is believed that synergism from the intercalated corrosion inhibitor and the clay leads to better corrosion protection than either nanoclay or corrosion inhibitor.

3.2 Hydrotalcite and Calcined Hydrotalcite Modification by Anionic Exchange

In the anionic exchange experiments with hydrotalcite (HT) and calcined hydrotalcite (CHT), only ionic liquid [THTDP][DE] was used as the organic modifier. From previous experiments (Kim 2006), it has been recognized that intercalation with small anions could not increase much the basal spacing. Therefore, [THTDP][DE] having a larger anion was evaluated for the anionic exchange modification. The abbreviations and experimental conditions are shown in Table 2.7.

3.2.1 Thermogravimetric Analysis

TGA results of unmodified hydrotalcite and hydrotalcite modified with the ionic liquid are shown in Figure 3.15. The dehydration of hydrotalcite takes place between 180°C and 300°C (Figure 3.15(a)). The thermal decomposition of carbonate ions to carbon dioxide and water takes place in the range of 350 - 500 °C, and the crystalline structure of HT-1 collapses by thermal decomposition at those temperatures.

The results for HT-3 show a smoother line at the temperature of the thermal decomposition of the carbonate ions and higher weight losses thereafter. Therefore, it can be assumed that the carbonate ion has been exchanged at least partly by the decanoate ion.

It was expected that the anionic exchange reaction of HT would be difficult because the hydrotalcite used in this research contains a strongly bonded carbonate anion. Therefore, a calcined hydrotalcite (CHT) was evaluated. CHT modification was based on the assumption that empty basal spacing of calcined hydrotalcite may be regenerated by ion exchange with ionic liquids. As a schematic regeneration process of calcined hydrotalcite is shown in Figure 3.14.

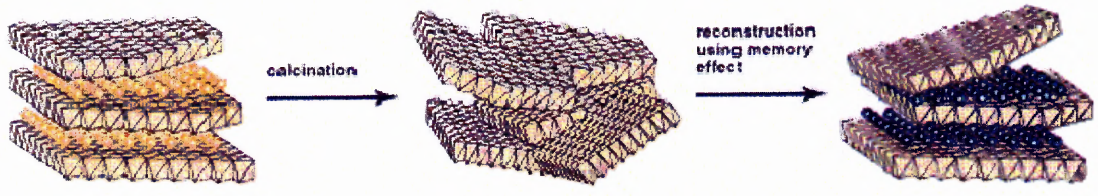

Figure 3.14 Regeneration process of calcined hydrotalcite.
(Li, Z. " Novel Solid Base Catalysts for Michael Additions Synthesis Characterization and Application", Ph.D. Dissertation, Humboldt University, Berlin, Germany, 2005).

The calcined hydrotalcite shows a different TGA pattern than pristine hydrotalcite. In Figure 3.16, CHT-1 does not show any dehydration between 180 and 300 °C or thermal decomposition between 350 and 500 °C. Hence, it is confirmed that carbonate ion and water have been removed by calcination. The TGA results of CHT-2 also do not indicate the presence of carbonate ion or water but rather the presence of an organic, temperature sensitive phase that may have been the decanoate anion.

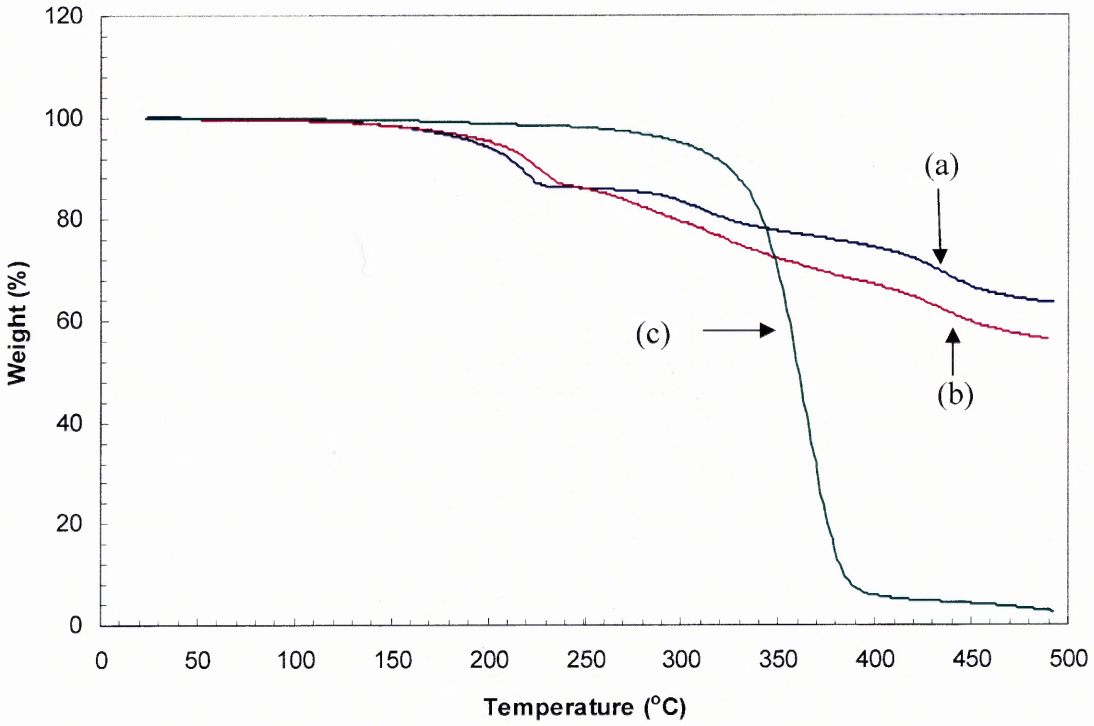

Figure 3.15 TGA results of (a) HT-1, (b) HT-3, and (c) [THTDP][DE].

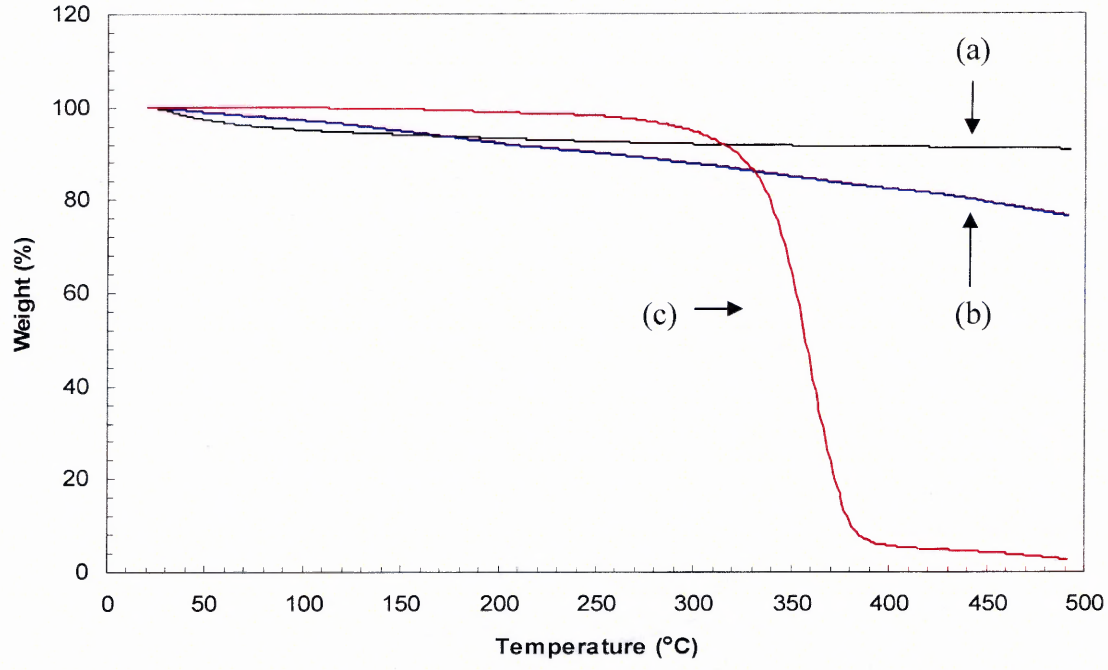

Figure 3.16 TGA results of (a) CHT-1, (b) CHT-2, and (c) [THTDP][DE].

3.2.2 Fourier Transform Infrared Spectroscopy

The FTIR spectra of HT-1 and HT-3 are shown in Figure 3.17. Although new peaks are observed around 2800 - 3000 cm^{-1} on HT-3, which may represent carbon-hydrogen stretching from the decanoate anion, the peak for the carbonate ion is still observed at 1360 cm^{-1}. Therefore, it is believed that the anion of the [THTDP][DE] is still present on the surface of the hydrotalcite.

Calcined hydrotalcite (CHT-1) and calcined hydrotalcite modified with [THTDP][DE] are shown in Figure 3.18. Unlike hydrotalcite (HT-1), calcined hydrotalcite (CHT-1) does not show any peaks in the range of 600 – 900 cm^{-1}. Modified calcined hydrotalcite (CHT-2) shows carbon hydrogen stretching between 2840cm^{-1} and 3000cm^{-1} which may have been created from the anionic exchange with the IL.

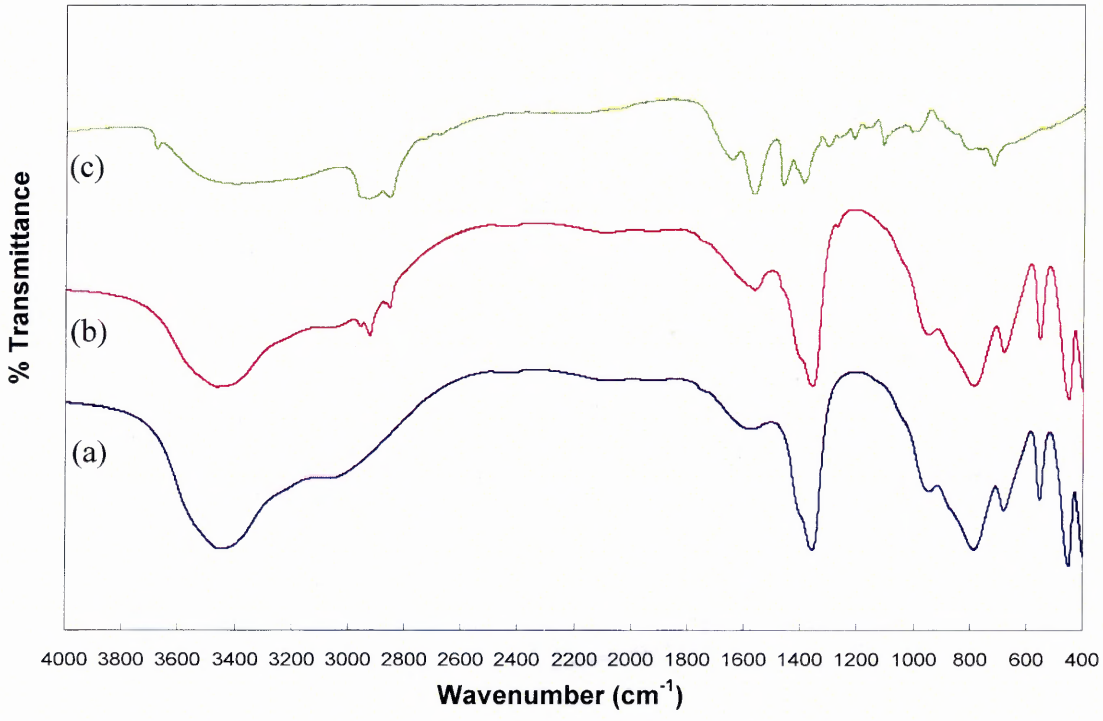

Figure 3.17 FTIR spectra of (a) HT-1, (b) HT-3, and (c) [THTDP][DE].

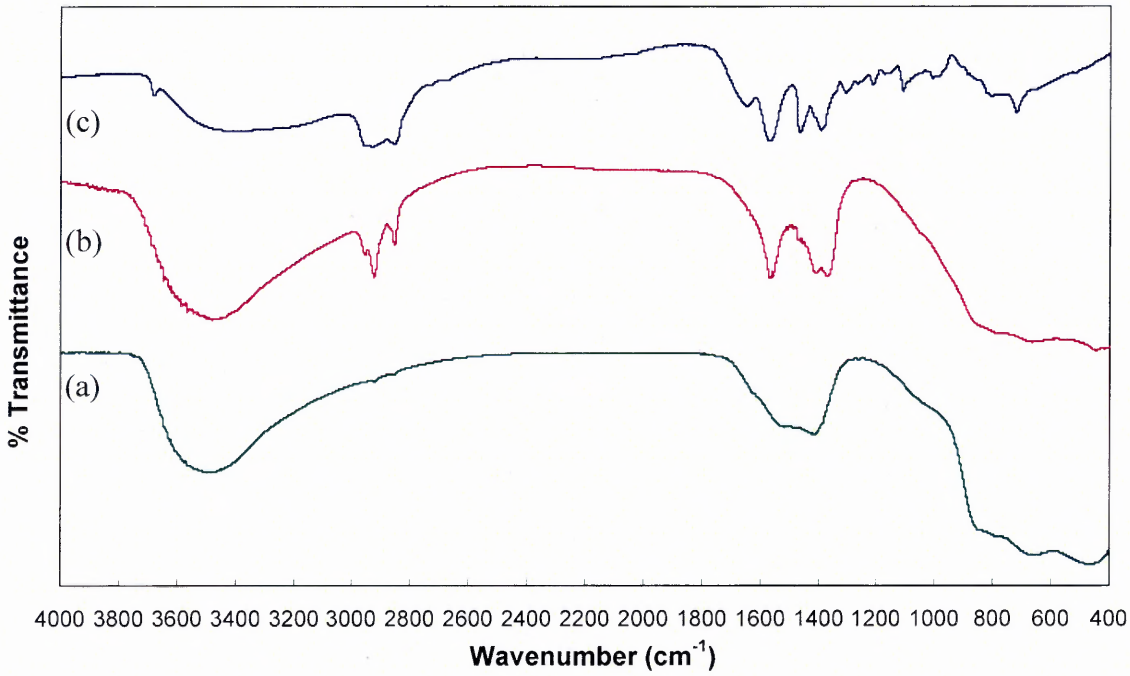

Figure 3.18 FTIR spectra of (a) CHT-1, (b) CHT-2, and (c) [THTDP][DE].

3.2.3 Wide Angle X-ray Diffraction

The anionic modification of hydrotalcite and calcined hydrotalcite with [THTDP][DE] did not increase the basal spacings as shown in Figure 3.19.

The WXRD results of HT-1 show a basal spacing of 0.756 nm ($2\theta = 11.71^{\circ}$), and HT-3 show a basal spacing of 0.765nm ($2\theta = 11.65^{\circ}$). Therefore, it is confirmed that the ionic liquid, [THTDP][DE], did not increase the interspacing of hydrotalcite either because a) the anion of IL is not large enough to increase the basal spacing. b) its orientation is unfavorable. c) it was not exchanged with the carbonate ion. The WXRD results of CHT-1 (Figure 3. 19(c)) show the amorphous characteristics of the calcined hydrotalcite since calcination collapses its structure. The WXRD results of CHT-2 (Figure 3.19 (d)) show a weak peak shifted only slightly from the original angle. Therefore, it appears that no intercalation took place but rather surface absorption.

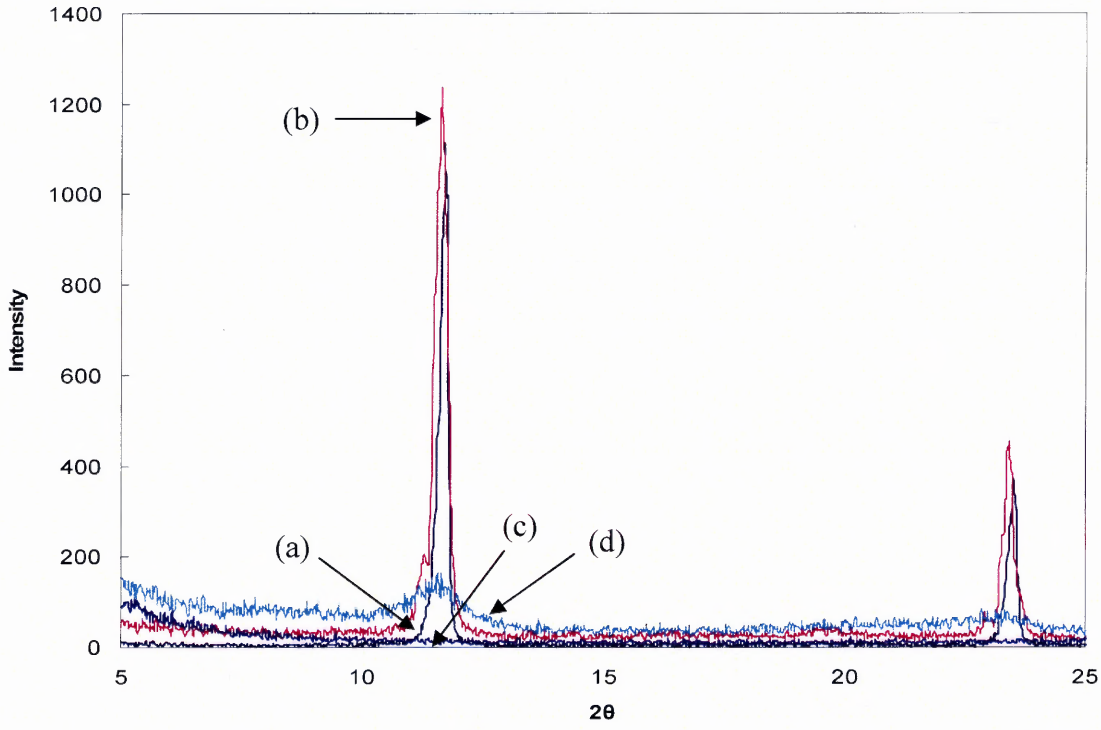

Figure 3.19 WXRD results of (a) HT-1, (b) HT-3, (c) CHT-1, and (d) CHT-2.

3.3 Polypropylene Nanocomposites with Modified Montmorillonites

3.3.1 Physiochemical Changes during Mixing

Polypropylene nanocomposites were prepared in a Brabender batch mixer. Experimental data are shown in Table 2.8. Figure 3.20 shows mixing data in terms of torque values and time. Slightly increased torque in PNC-2, PNC-3, and PNC-4 correspond to the time when fillers were added. Unlike the previous nanocomposites (Kim et al. 2006, Appedix A) modified with [EMIM][Br], [HXMIM][Cl] and commercial clays, the torques of nanocomposites modified with phosphonium based ILs are continuously stable until the end of mixing. This is presumably the result of the higher thermal stability of the phosphonium based ionic liquids used for MMT-6 and MMT-7.

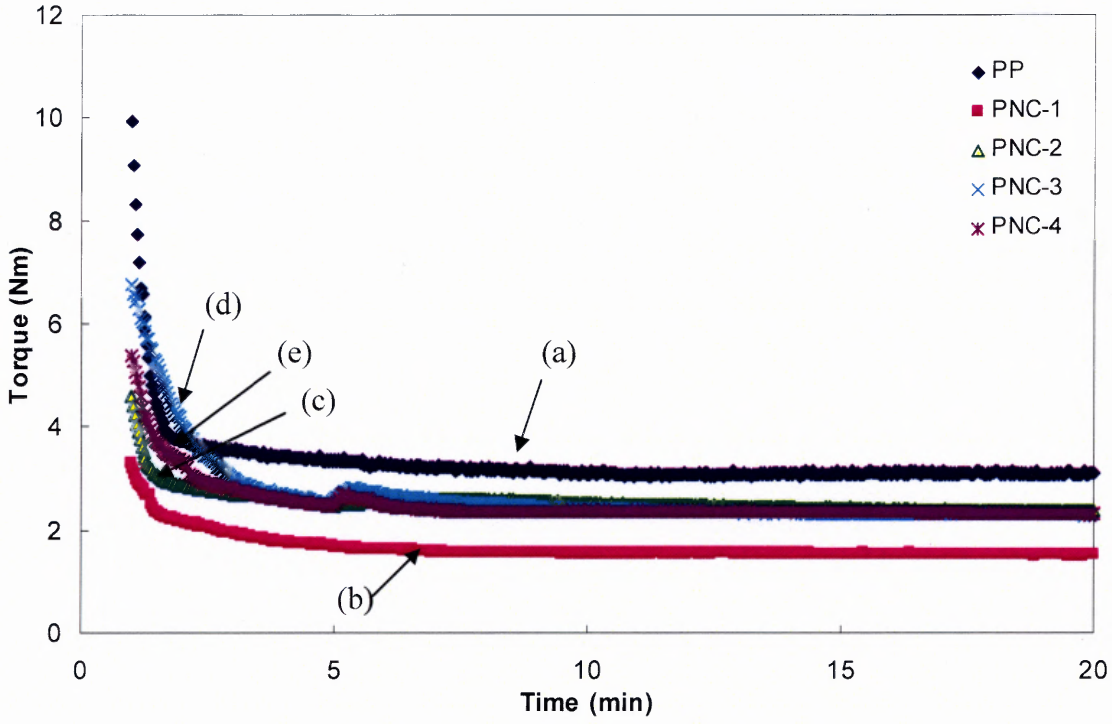

Figure 3.20 Batch mixing data of polypropylene nanocomposites (a) PP, (b) PNC-1, (c) PNC-2, (d) PNC-3, and (e) PNC-4.

After batch mixing, composites were used for making thin disk films in order to determine dispersion from visual differences. As shown in Figure 3.21, nanocomposite disks made from PNC-3 and PNC-4 do not show any agglomeration of the nanoclays in the polymer matrix. However, nanocomposites made from MMT modified with [HXMIM][Cl] (PN-5) and [Etpy][BF_4] (PN-6) show some agglomerated nanoclay particles. PNC-4 and PN-6 were made from nanoclays modified with ILs which have the same anion. However, PNC-4 shows better dispersed morphology than PN-6 due to the presence of a larger and hydrophobic cation ([$THTDP^+$] vs [$Etpy^+$]).

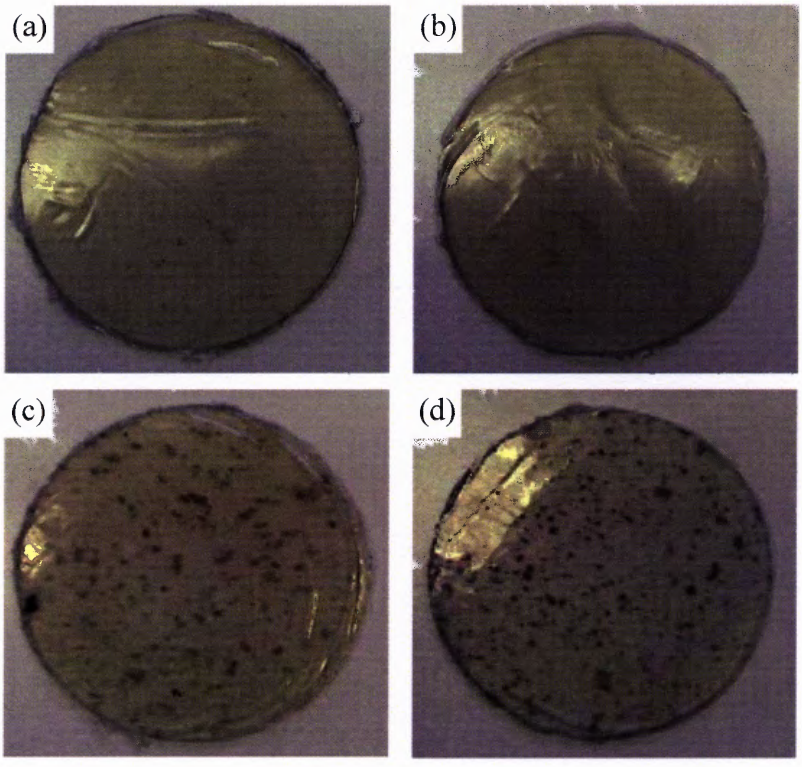

Figure 3.21 Thin disks of nanocomposites (a) PNC-3, (b) PNC-4, (c) PN-5 and (d) PN-6 (PN-5 and PN-6 were previously made from the MMT modified with [HXMIM][Cl] and [Etpy][BF_4], respectively [Kim et al. 2006]).

3.3.2 Scanning Electron Microscopy

Thin disks of nanocomposites were used to prepare samples for scanning electron microscopy. Frozen disks were cut immediately after 5 minutes immersion in liquid nitrogen, and broken surfaces of the samples were observed by SEM. A nanocomposite (PNC-2) containing unmodified clay is shown in Figure 3.22. The image shows agglomerated clay particles of a tactoid structure. PN-5 shown in Figure 3.25 also indicates a tactoid structure. However, PNC-3 and PNC-4 which are shown in Figure 3.23 and 3.24, respectively, have better dispersed morphologies. Although nanoclays in PNC-3 and PNC-4 still form some agglomerates, they are well dispersed over the entire

cross sectional area compared to the previous nanocomposites modified with lower molecular weight ILs [Kim et al 2006].

SEM images of agglomerates of MMT-6 and MMT-7 dispersed in PNC-3 and PNC-4, respectively, have thickness of around 1μm (Appendix A). On the other hand, PN-5 and PN-6 containing previously used ILs show larger agglomerates than PNC-3 and PNC-4 (Appendix A) of present study. A polypropylene composite mixed with a commercial clay (Cloisite® 15A) shows the best dispersed morphology (Figure 3.26). According to manufacturer's data, the basal spacing of Closite® 15A is about 3.15 nm which is almost twice the spacing of the modified clays in this research. Therefore, it can be confirmed that expanding the basal spacing with the proper organophobic cation plays a key role in dispersing the clays in the polyolefin matrix.

Figure 3.22 SEM image of PNC-2.

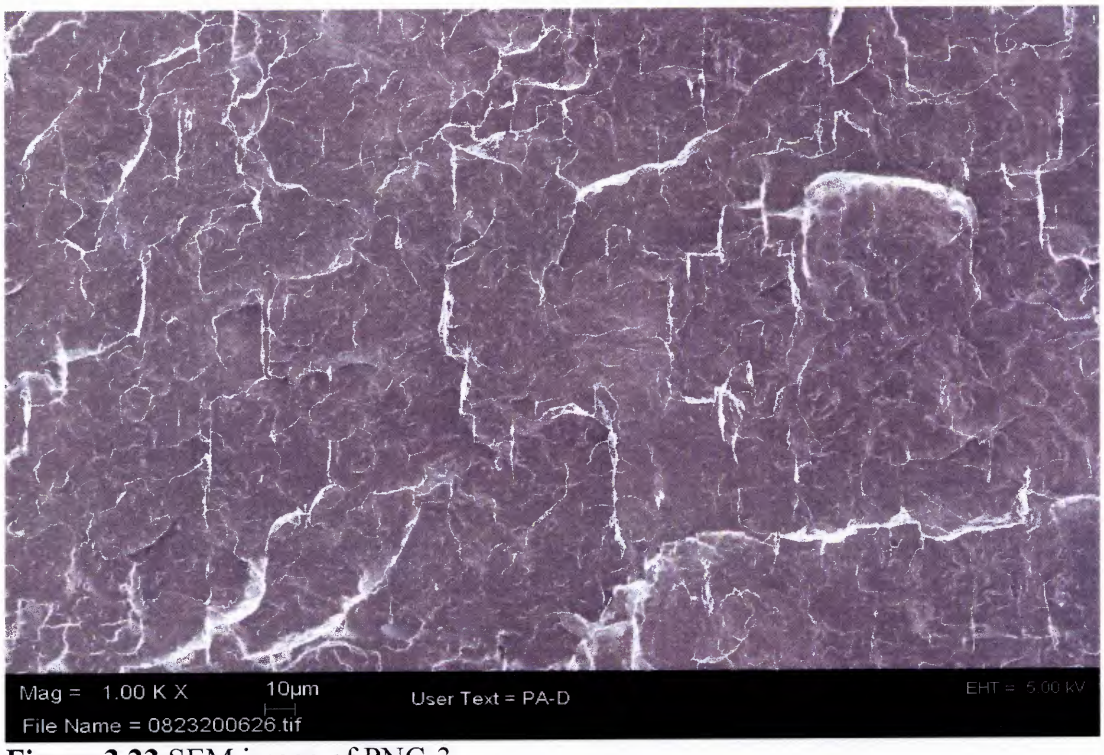

Figure 3.23 SEM image of PNC-3.

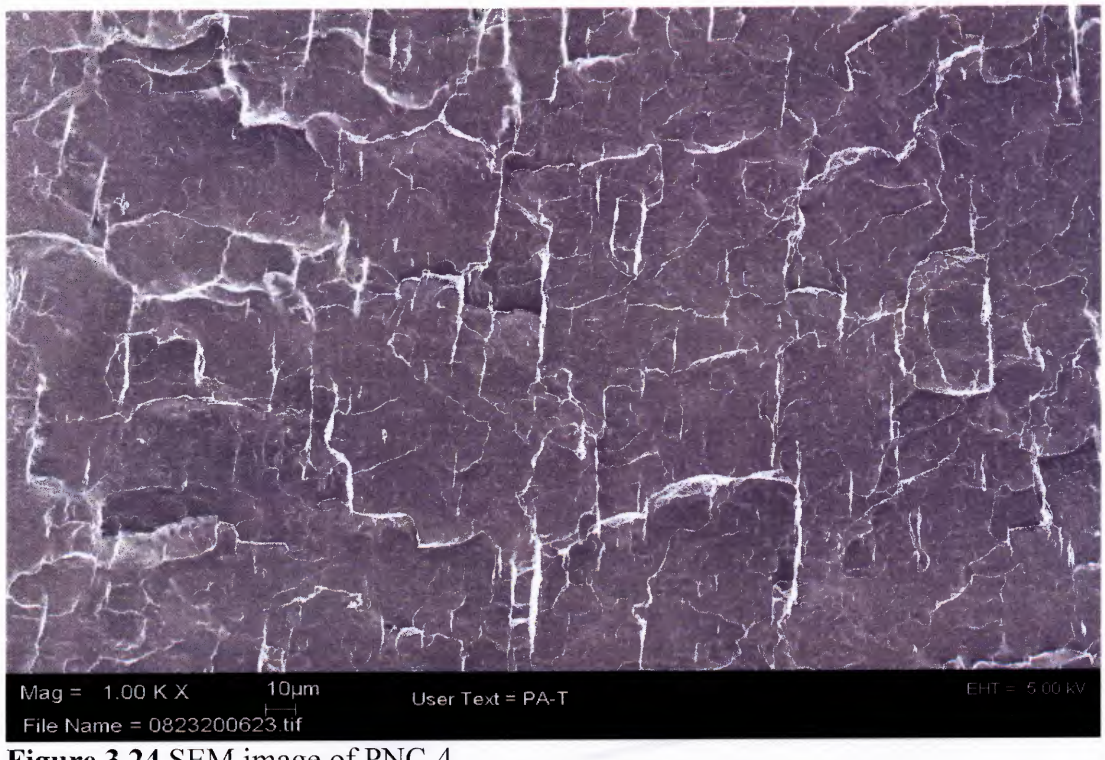

Figure 3.24 SEM image of PNC-4.

Figure 3.25 SEM image of PN-5.

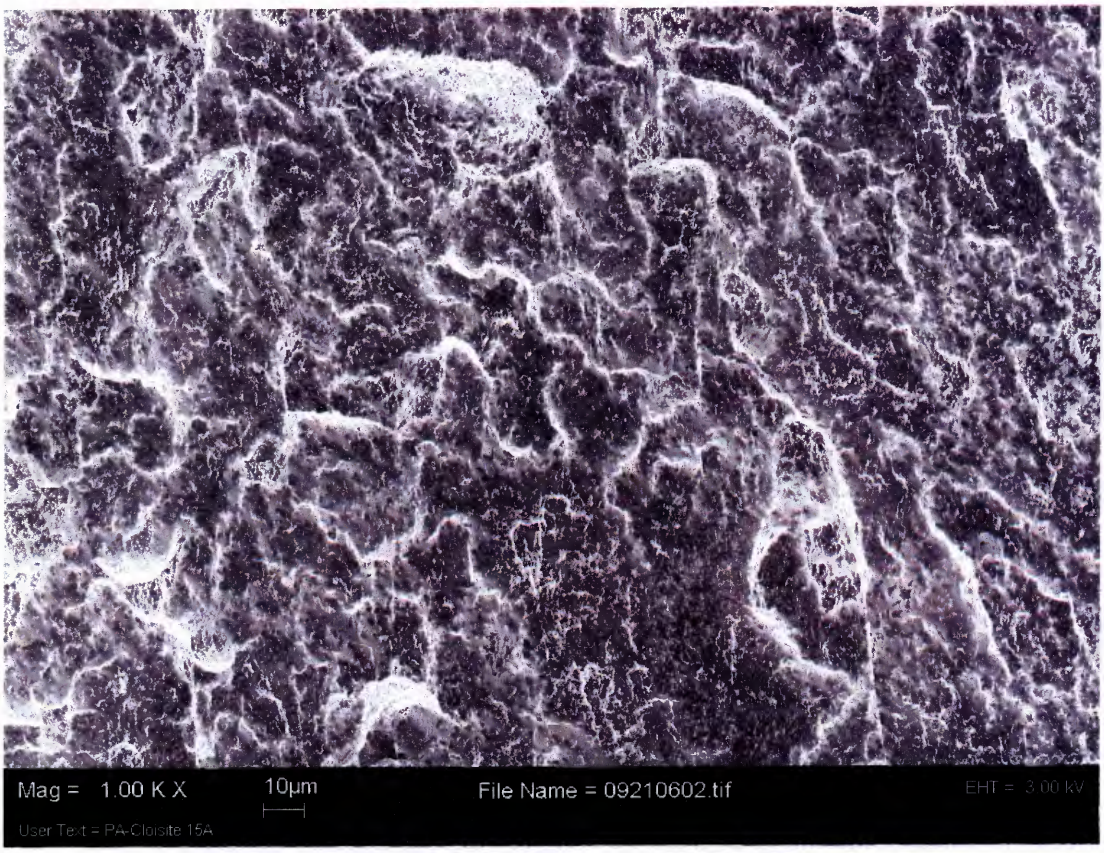

Figure 3.26 SEM image of PNC-15A.

3.3.3 Transmission Electron Microscopy

Modified clays and unmodified clays in the polypropylene matrix were observed by transmission electron microscopy. The dark lines of the TEM images in Figure 3.27 represent the layers of the nanoclays.

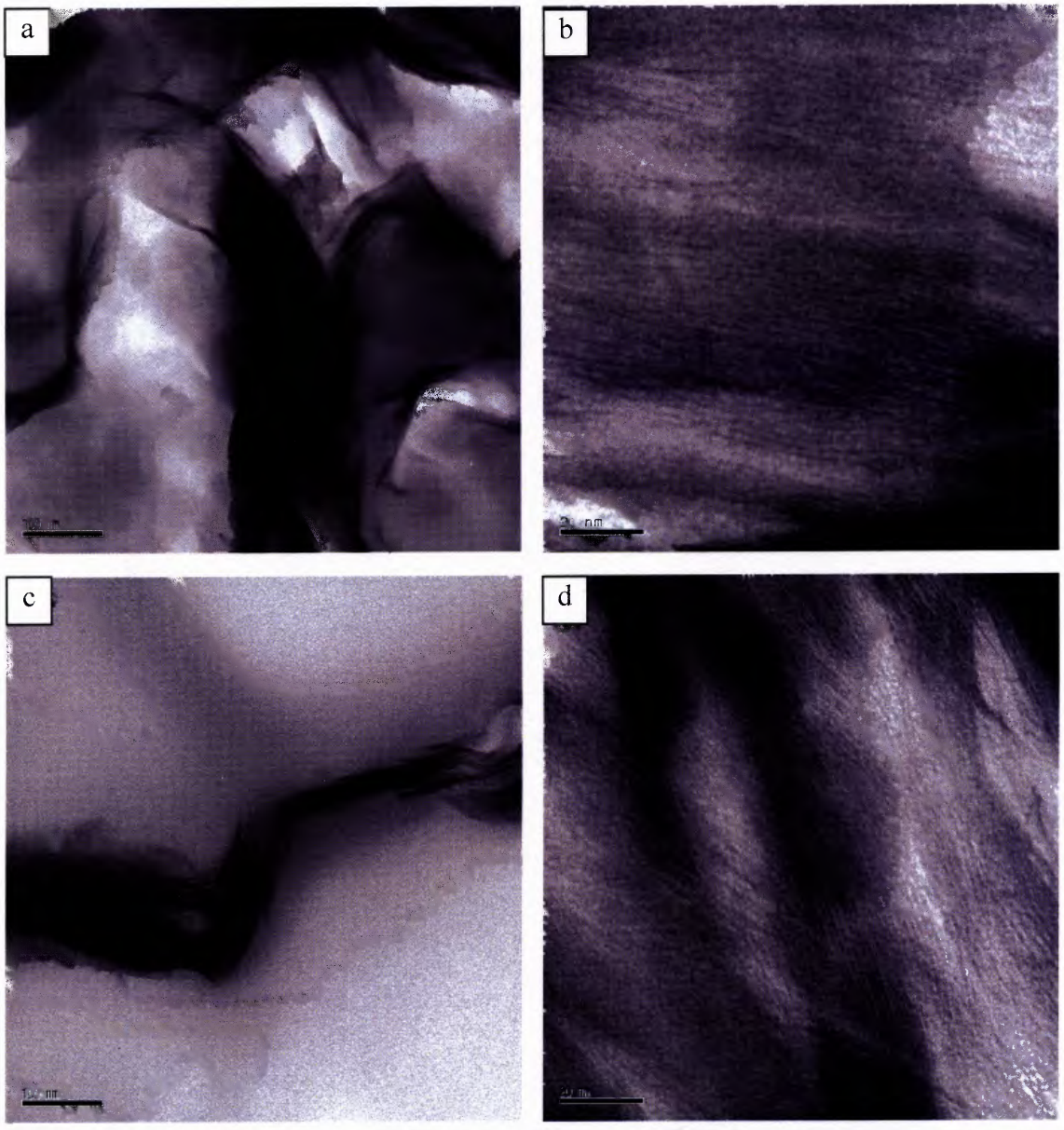

Figure 3.27 TEM image of (a) PNC-2, (b) PNC-3, (c) PNC-3 and (d) PNC-4.

Figure 3.27 (a) shows a TEM image of MMT-1 in PP representing a common tactoid structure of nanoclays in a polymer matrix. The other images (Figure 3.27 (b), (c) and (d)) are modified MMTs in PP composites showing partially intercalated or tactoid structures. In Figure 3.27 (b), the modified clays roughly contain ten lamellae in the thickness of 20 nm. This is approximately consistent with the XRD results (MMT-6: 1.82 nm, MMT-7: 1.87 nm) reported earlier.

APPENDIX A

CATIONIC MODIFICATION OF MONTMORILLONITE

In this Appendix, additional SEM images of nanocomposites at different magnifications, TGA results at different times and temperatures and batch mixing data from previous experiments are shown.

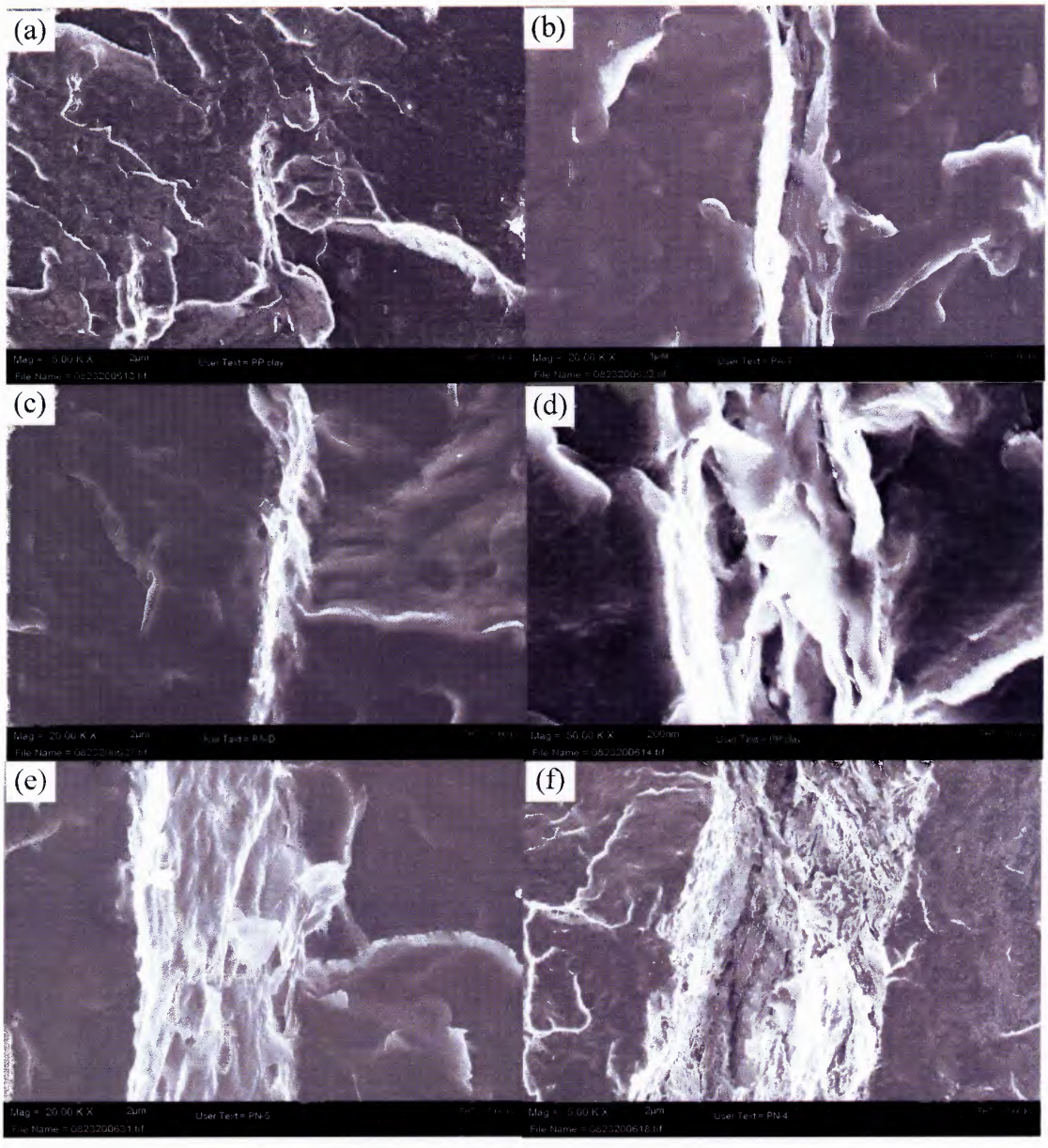

Figure A.1 SEM images of nanocomposites (a) PNC-2, (2) PNC-4, (c) PNC-3, (d) PNC-2 (e) PN-5 and (f) PN-6.

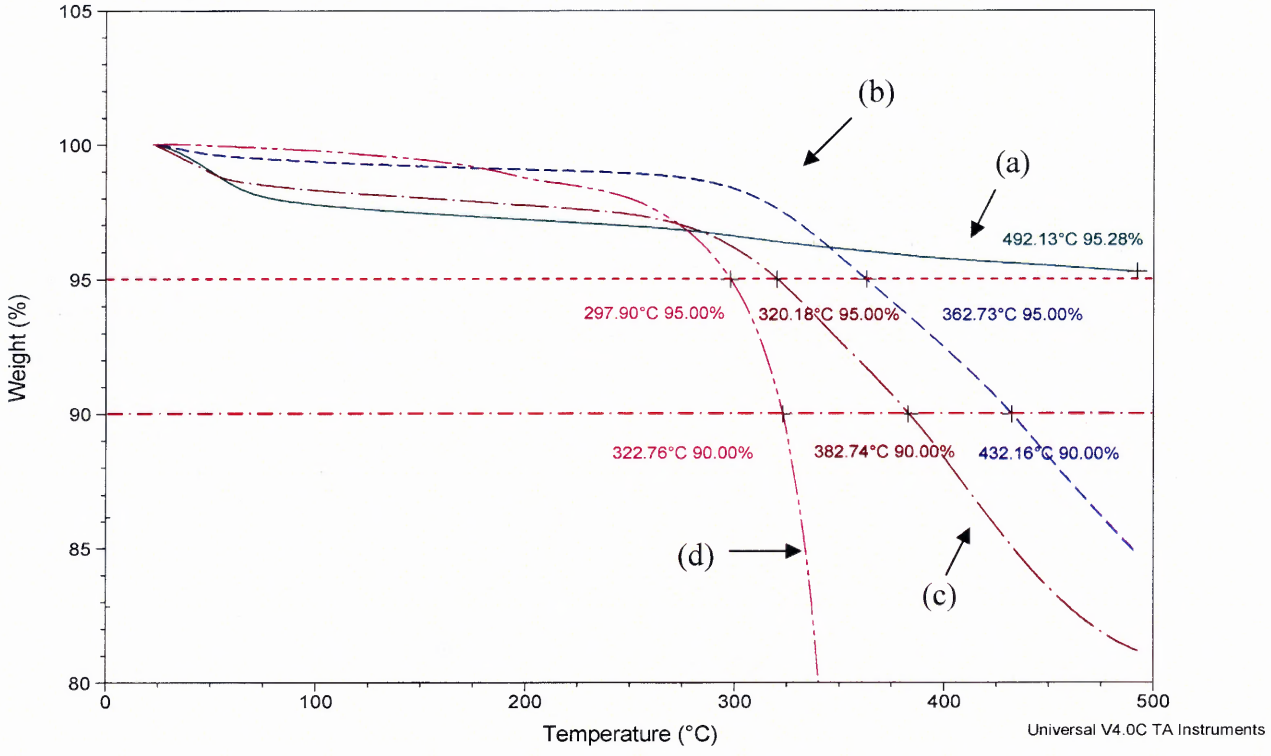

Figure A.2 TGA results of (a) MMT-1, (b) MMT-2, (c) MMT-6 and (d) [THTDP][DE].

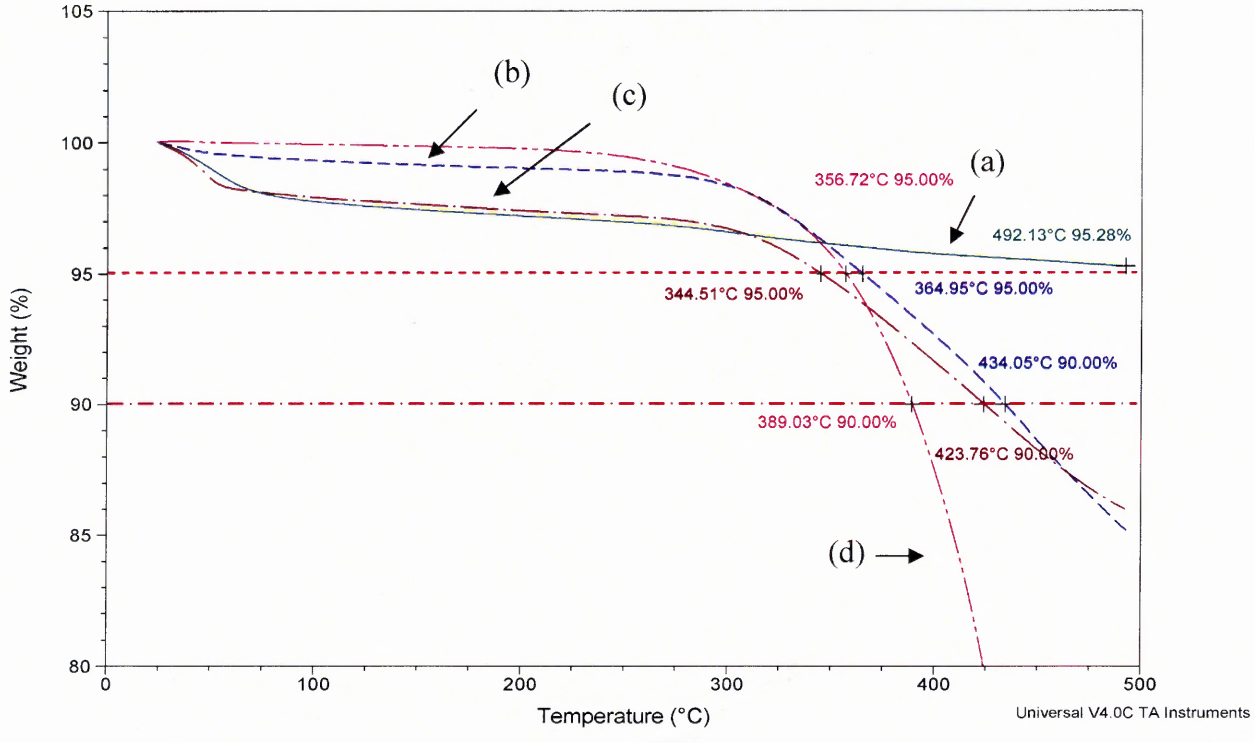

Figure A.3 TGA results of (a) MMT-1, (b) MMT-3 (c) MMT-7 and (d) [THTDP][BF_4].

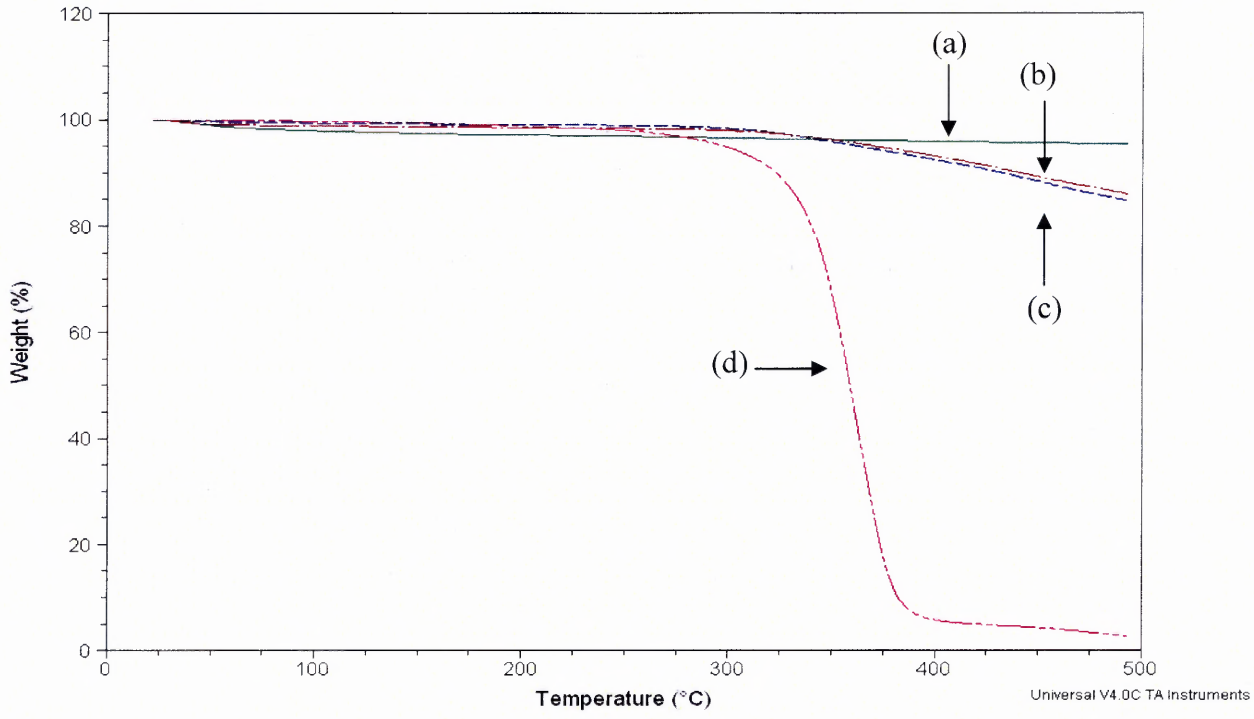

Figure A.4 TGA results of (a) MMT-1 (b) MMT-2 (c) MMT-4 and (d) [THTDP][DE].

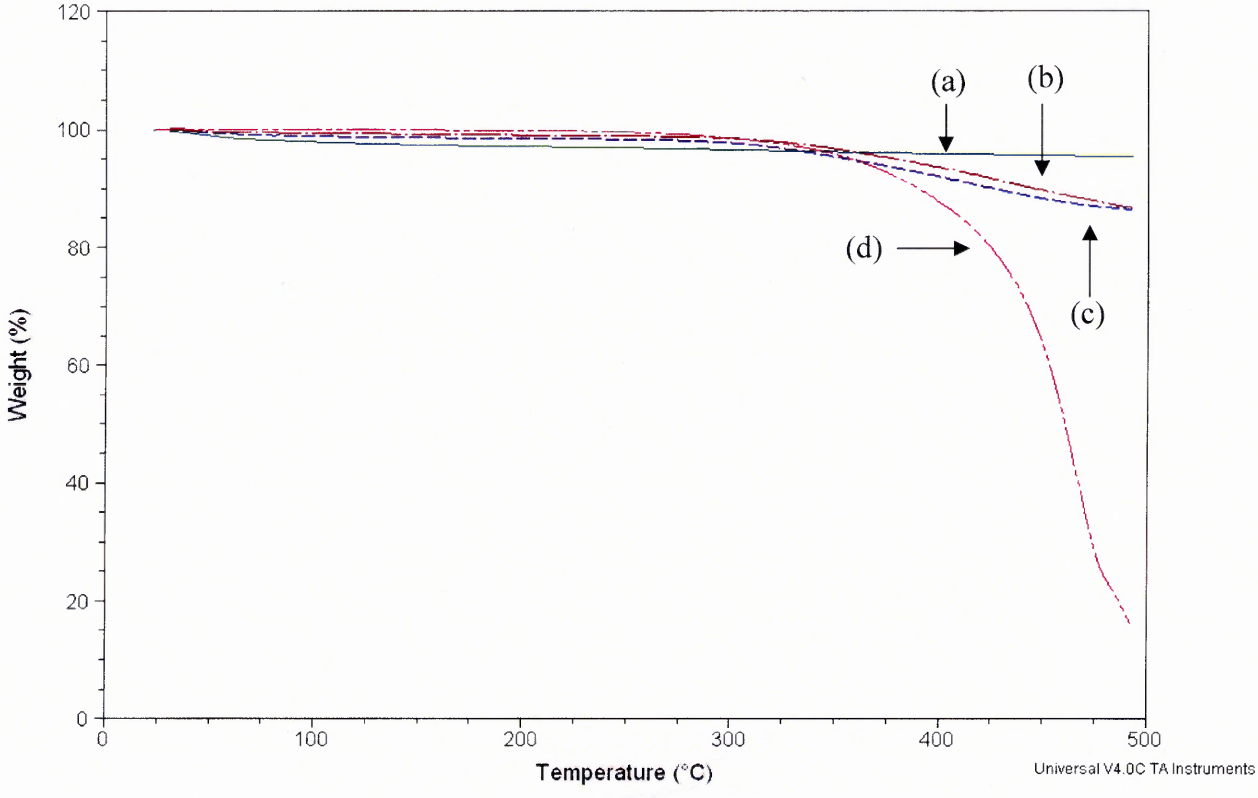

Figure A.5 TGA results of (a) MMT-1, (b) MMT-3, (c) MMT-5, and (d) [THTDP][BF_4].

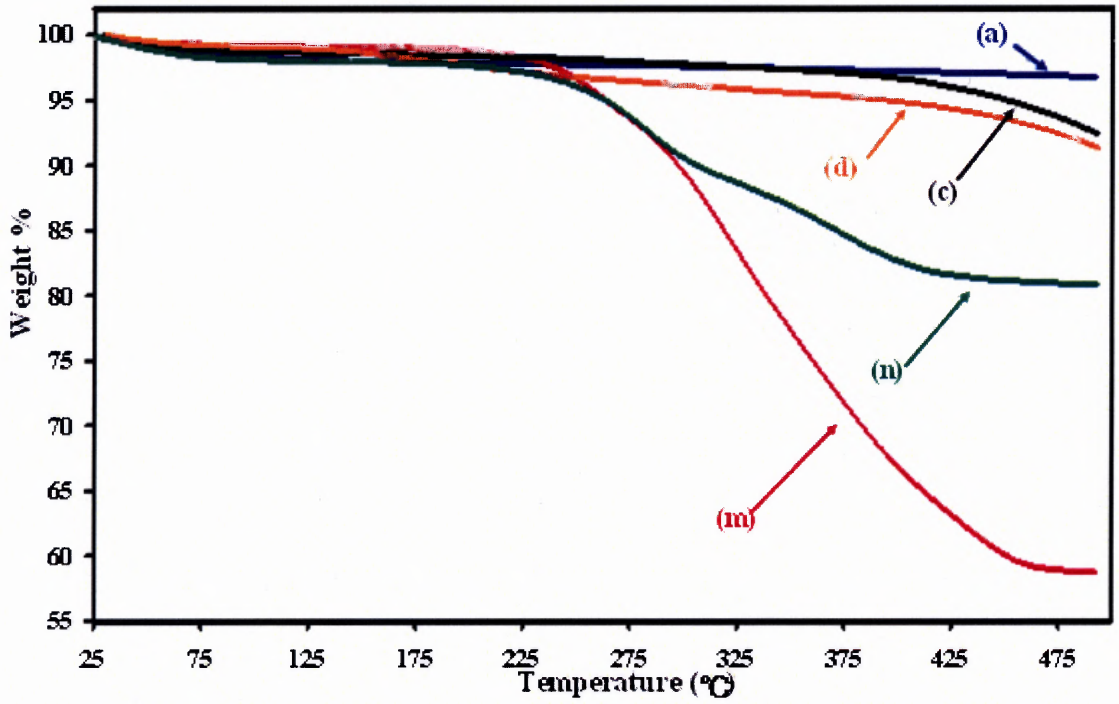

Figure A.6 TGA results of (a) Clay-1, (c) Clay-3, (d) Clay-5, (m) Cloisite® 15A (n) Cloisite® 30B [Kim et al. 2006].

Table A.1 Additional Information Regarding Figure A.6

Abbreviations	Nanoclays	Organic Modifiers
Clay-1	MMT-Na^+	-
Clay-3	MMT-Na^+	1X [EMIM][Br]
Clay-5	MMT-Na^+	2X [EMIM][Br]
Cloisite® 15A	MMT-Na^+	2M2HT
Cloisite® 30B	MMT-Na^+	EM2EtOH

(Source: Kim et al, *Microporous Mesoporous Mater.*, **2006**, 96, 26-35.)

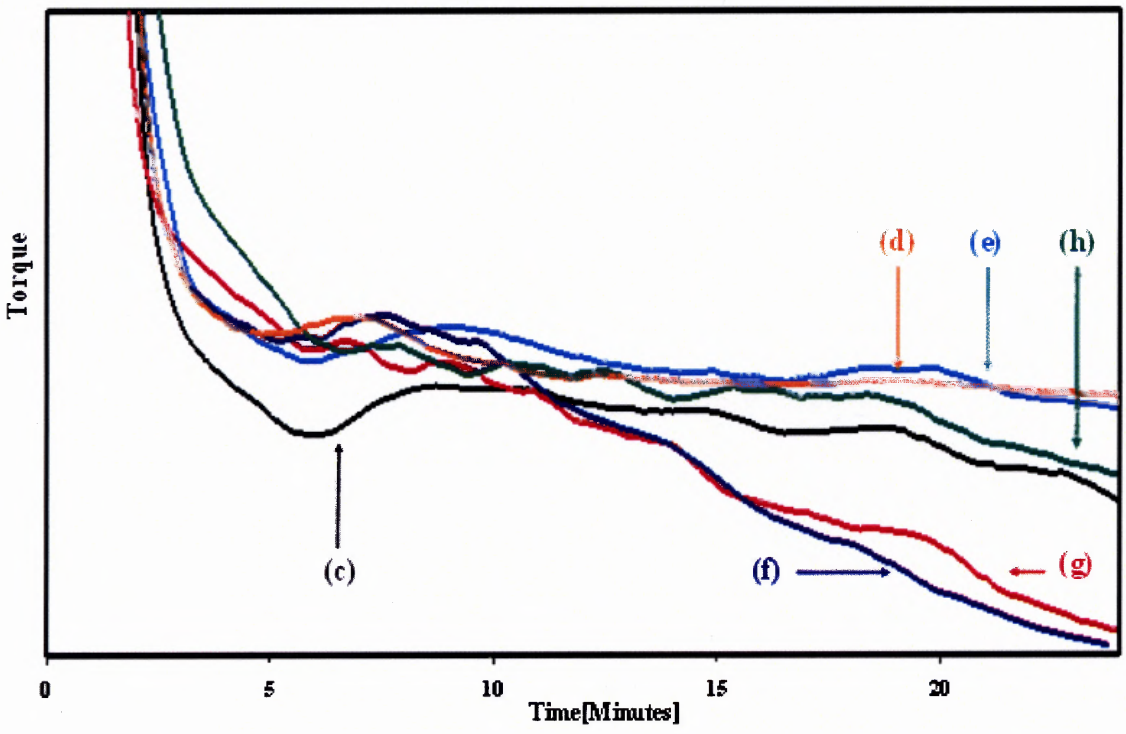

Figure A.7 Batch mixing data of polypropylene nanocomposites (c) PN-1, (d) PN-2, (e) PN-3, (f) PN-4, (g) PN-5, and (h) PN-6 [Kim et al. 2006].

Table A.2 Additional Information Regarding Figure A. 7

Abbreviations	Nanoclays	Polymers	Organic Modifiers
PN-1	MMT-Na^+	PP + PP-g-MA	-
PN-2	MMT-Na^+	PP + PP-g-MA	2M2HT
PN-3	MMT-Na^+	PP + PP-g-MA	MT2EtOH
PN-4	MMT-Na^+	PP + PP-g-MA	[EMIM][Br]
PN-5	MMT-Na^+	PP + PP-g-MA	[HXMIM][Cl]
PN-6	MMT-Na^+	PP + PP-g-MA	[Etpy][BF_4]

(Source: Kim et al, *Microporous Mesoporous Mater.*, **2006**, 96, 26-35.)

APPENDIX B

ANIONIC MODIFICATION OF HYDROTALCITE

In this Appendix, additional SEM images are shown in Figure B.1 and Figure B.2 for HT and CHT systems. TGA results at different treatment times are shown in Figure B.3.

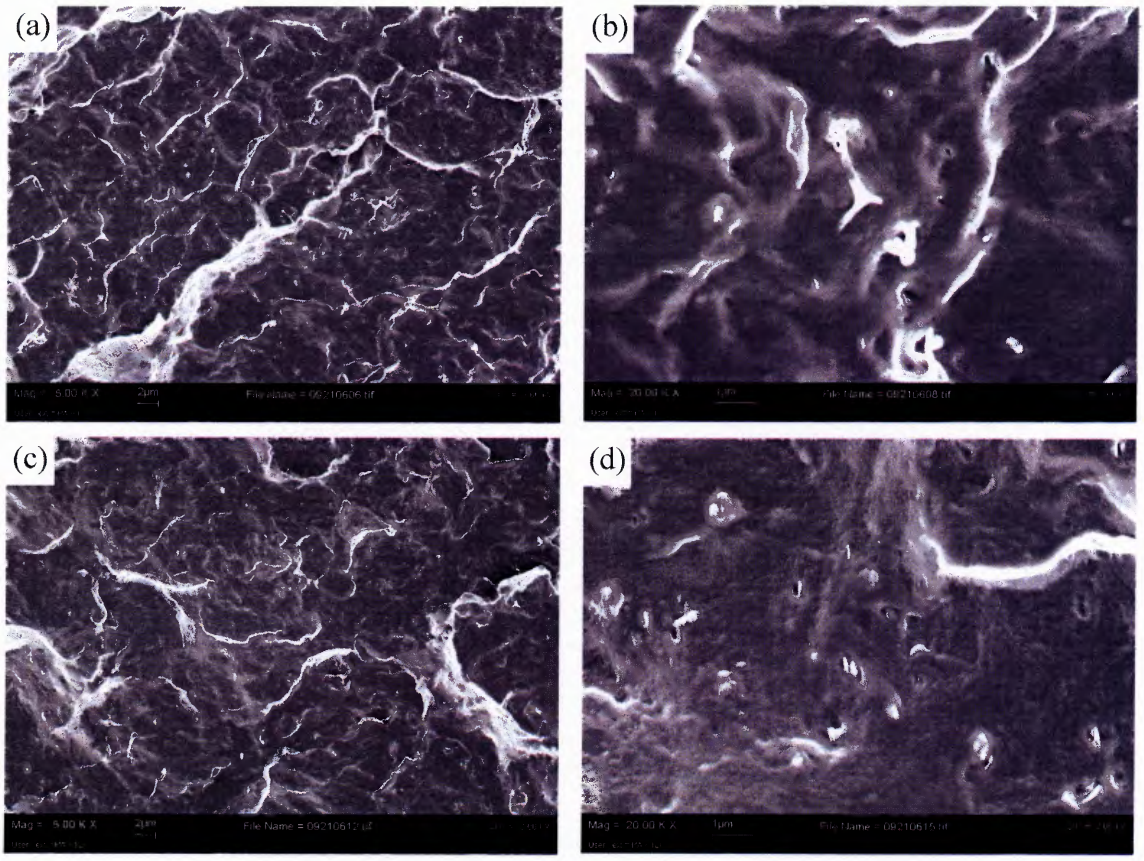

Figure B.1 SEM images of nanocomposites (a) HT-1, (b) HT-1, (c) HT-3 and (d) HT-3.

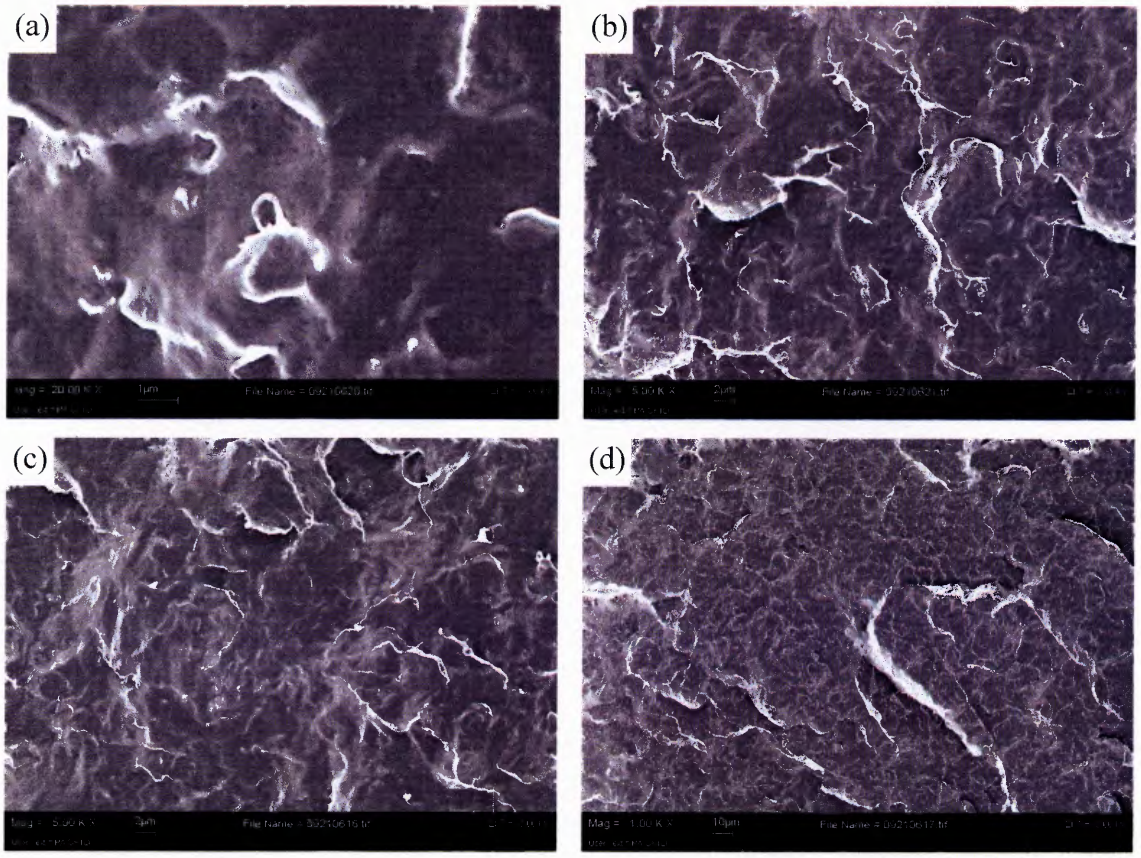

Figure B.2 SEM images of CHT-2 at different magnifications.

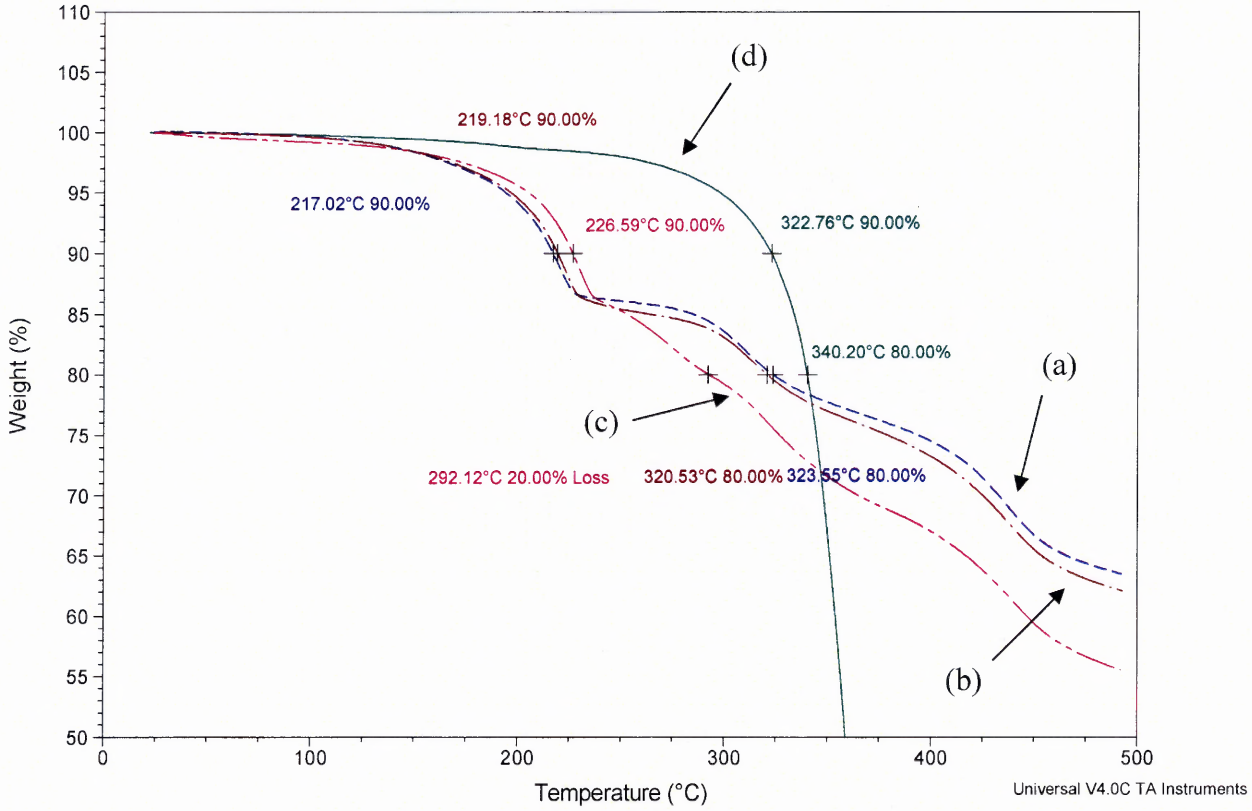

Figure B.3 TGA results of (a) HT-1, (b) HT-2, (c) HT-3 and (d) [THTDP][DE].

REFERENCES

Alexandre, M.; Dubois, P. "Polymer-Layered Silicate Nanocomposites: Preparation, Properties and Uses of New Class of Materials", *Material Science and Engineering*, **2000**, *28*, 1- 63.

Blumstein, A. "Polymerization of Adsorbed Monolayers / Thermal Degradation of The Inserted Polymer", *Journal of Polymer Science Part A: General Papers,* **1965**, *3* 2665 - 2672.

Bonnet, L. G.; Kariuki, B. M. "Ionic liquids: Synthesis and Characterisation of Triphenylphosphonium Tosylates", *European Journal of Inoragnic Chemistry,* **2006**, *2,* 437- 446.

Bradaric, C. J.; Downard, A.; Kennedy, C.; Robertson, A. J. Zhou, Y. "Industrial Preparation of Phosphonium Ionic Liquids", *Green Chemistry,* **2003**, *5*, 143-152.

Buchheit, R. G.; Wong, F. "Active Corrosion Protection and Corrosion Sensing in Chromate-Free Organic Coatings", *Progress in Organic Coatings*, **2003**, *47*, 174 - 182.

Byrne, C.; McNally, T.; Armstrong, C. G. "Thermally Stable Modified Layered Silicates for PET Nanocomposites.", *PPS 2005 Americas Regional Meeting Proceedings.* (2005).

Carrado, K. A. " Introduction: Clay Structure, Surface Acidity, and Catalysis", *Handbook of Layered Materials*, Edited by Auerbach S. M.; Carrado K. A., Marcel Dekker Inc., New York 2004, pp. 1-37.

Chiappe, C.; Pieraccini, D. "Ionic liquids: Solvent Properties and Organic Reactivity", *Journal of Physical Organic Chemistry*, **2005**, *18*, 275-297.

Choy, J.; Park, M. "Cationic and Anionic Clays for Biological Applications", *Clay Surfaces*, Edited by Wypych F. and Satyanarayana K. G., Elsevier, Oxford, U.K. 2004, pp. 403-424.

Cook, R. L.; Myers, A.; Elliott, J; Noce, J; Garland, G. "Smart Corrosion Inhibiting Coatings from Nanoparticle Additives", *Polymeric Materials: Science & Engineering*, **2006**, *51*, 88 -99.

Fujiwara, S.; Sakamoto, T. Japanese Kokai Patent Application No. 109998; Assigned to Unitika KK, Japan (1976).

Gao, F. "Clay/Polymer Composites: The Story", *Materials Today*, **2001**, *20*, 50 - 55.

Giannelis, E. P.; Shah, D.; Schmidt, D. "New Advances in Polymer Layered Silicate Nanocomposites", *Current Opinion in Solid State & Materials Science,* **2002**, *6*, 205-212.

Gilman, J. W.; Jackson, C.; Morgan, A. B.; Harris, R. Jr.; Manias, E.; Giannelis, E. P. "Flammability Properties of Polymer Layered silicate Nanocomposites: Polypropylene and Polystyrene Nanocomposites", *Chemistry Materials*, **2000**, *12*, 1866-1873.

Gopakumar, T. G.; Patel, N. S.; Xanthos, M. "Effect of Nanofillers on the Properties of Flexible Protective Polymer Coatings", *Polymer Composites,* **2006**, *27*, 368-380.

Gordon, C. M. " New Developments in Catalysis Using Ionic Liquids", *Applied Catalysis,* **2001**, *222*, 101-117.

Grim, R. E. "Clay Mineralogy", McGraw-Hill Book Co. Inc., New York, 1968.

Huddleston, J. G.; Visser, A. E.; Reichert, M. W. Willauer, H. D.; Broker, G. A.; Rogers R. D. "Characterization and Comparison of Hydrophilic and Hydrophobic Room Temperature Ionic Liquids Incorporating the Imidazolium Cation", *Green Chemistry*, **2001**, *3*, 156-164.

Jeon, H. G.; Jung, H. T.; Lee, S. W.; Hudson S. D. "Morphology of Polymer Silicate Nanocomposites" *Polymer Bulletin,* **1998**, *41*, 107-113.

Kamena, K. "Nanoclays and Their Emerging Markets", *Functional Filler for Plastics*, Edited by Xanthos M., 163-171, Wiley-VCH: Weinheim, Germany, (2005).

Karol, M. "A Method of Calculations of The Parameters in The Vogel Tammann Fulcher's Equation: An Application to The Porcine Serum Albumin Aqueous Solutions", *Current Topics in Biophysics*, **2003**, *27*, 17-21.

Kato, M.; Usuki, A.; Okada, A. "Synthesis of PP Oligomer Clay Intercalation Compounds." *Journal of Applied Polymer Science*, **1997**, *66*, 1133-1138.

Kim, N. H. "Modification of Clays with Ionic Liquids for Polymer Nanocomposites" Master Thesis, New Jersey Institute of Technology, Newark, NJ, **2006**

Kim, N. H.; Malhotra, S. V.; Xanthos M. "Modification of Cationic Nanoclays with Ionic Liquids" *Microporous and Mesoporous Materials*, **2006**, *96*, 29-35.

Kooli, F.; Jones, W "Direct Synthesis of Polyoxovanadate-Pillared Layered Double Hydroxides.", *Inorganic Chemistry,* **1995**, *34*, 6237-6249.

Lan, T.; Kaviratna, P.D.; Pinnavaia, T. J. "On the Nature of Polyimide-Clay Hybrid Composites, *Chemistry Materials*, **1994**, *6*, 573-575.

Landolt, D. "Introduction to Surface Reactions" *Corrosion Mechanisms in Theory and Practice*, Edited by Marcus, P., Marcel Dekker Inc.: New York, 2002 pp. 1- 48.

Li, Z. " Novel Solid Base Catalysts for Michael Additions Synthesis Characterization and Application", Ph.D. Dissertation, Humboldt University, Berlin, Germany, 2005.

Lin, Y.; Wang, J.; Evans, D. G.; Li, D. "Layered and Intercalated Hydrotalcite-like Materials as Thermal Stabilizers in PVC Resin." *Journal of Physics and Chemistry of Solids,* **2006**, *67*, 998-1001.

Liu, L.; Qi, Z.; Zhu, X. "Studies on Nylon-6 Clay Nanocomposites by Melt-Intercalation Process." *Journal of Applied Polymer Science,* **1999**, *71*, 1133-1138.

Musto, P.; Ragosta, G.; Scarinzi, G.; Mascia, L. "Polyimide-Silica Nanocomposites: Spectroscopic, Morphological and Mechanical Investigation." *Polymer,* **2004**, *45*, 1697 - 1706.

Newman, S. P.; Jones, W. "Synthesis, Characterization and Applications of Layered Double Hydroxides Containing Organic Guests" *New Journal of Chemistry*, **1998**, 22, 105-115.

Ngo, H. L.; LeCompte, K.; Hargens, L.; McEwen, A. B. "Thermal Properties of Imidazolium Ionic Liquid" *Thermochimica Acta*, **2000**, *357*, 97-102.

Qutubuddin, S.; Fu, X. "Polymer-clay nanocomposite: synthesis and properties" Nanosurface Chemistry Edited by Rosoff M., Marcel Dekker Inc.: New York, 2002, pp. 653-673.

Reichle, W. T. "Synthesis of Anionic Clay Minerals", *Solid State Ionics*, **1986**, *22,* 135-141.

Reijers, H. T. J.; Valster-Schiermeier, S. E. A.; Cobden, P. D.; van den Brink, R. W. "Hydrotalcite as CO_2 Sorbent for Sorption-Enhanced Steam Reformaing of Methane", *Industrial and Engineering Chemistry Research*, **2006**, 45, 2522-2530.

Reijers, H. T. J.; Elzinga, G. D. ; Kluiters, S. C. A.l Dijkstra, J. W; Cobden, P. D.; van den Brink, R. W. "Sorption-Enhanced Reaction Process for Electricity Production and CO_2 Capture" AIChE Annual Meeting, Conference Proceedings, Cincinnati, OH, Oct.30 - Nov. 4, 2005.

Snedden, P.; Winterton, N. "Cross-Linked Polymer Ionic Liquid Composite Materials", *Macromolecules,* **2003**, *36*, 4549-4556.

Southern Clay Product Inc., Gonzales, USA, Typical Physical Properties Bulletin Cloisite-Na^+, 2005.

Stoeffler, K.; Lafleur, P. G.;Denault, J. "Thermal Properties of Polyethylene Nanocomposites based on Different Organoclays", SPE Annual Technical Conference Proceedings, 263-267 Charlotte, NC, May 7- 11, 2006.

Usuki, A.; Tukigase, A.; Kato M. "Preparation and Properties of EPDM-clay hybrids", *Polymer,* **2002**, *43*, 2185-2189.

Usuki, A.; Kato, M.; Okada, A.; Kurauchi, T. "Synthesis of Polypropylene Clay Hybrid", *Journal of Applied Polymer Science*, **1997**, *63*, 137-139.

Vaccari, A. "Preparation and Catalytic Properties of Cationic and Anionic Clays", *Catalysis Today,* **1998**, *41*, 53-71.

Vaia, R. A.; Giannelis, E. P. "Lattice Model of Polymer Melt Intercalation in Organically Modified Layered Silicates", *Macromolecules*, **1997**, *30*, 7990-7999.

Vaia, R. A.; Giannelis, E. P. "Polymer Melt Intercalation in Organically Modified Layered Silicates", *Macromolecules*, **1997**, *30*, 8000-8009.

Vaia, R. A.; Teukolsky, R. K.; Giannelis E. P. "Interlayer Structure and Molecular Environment of Alkylammonium Layered Silicates", *Chemistry Materials*, **1994**, *6*, 1017-1029.

Wang, G. A.; Wang, C. C. et al. "The Disorderly Exfoliated LDHs/PMMA Nanocomposites Synthesized by In Situ Bulk Polymerization: the Effect of LDH-U on Thermal and Mechanical Properties" *Polymer Degradation and Stability,* **2006**, *91*, 2443-2450.

Wikipedia, " Information of corrosion inhibitor", Retrieved September, 2006 from the World Wide Web: http://en.wikipedia.org/wiki/Corrosion_inhibitor

Xanthos, M. "Polymers and Fillers", Functional Fillers for Plastics, edited by Xanthos, M., Wiley-VCH, Weinheim: Germany 2005, pp. 3-38.

Xu, W.; Cooper, E. I.; Angell C. A. " Ionic Liquids: Ion Mobilities, Glass Temperature, and Fragilities." *Journal of Physical Chemistry Part B*, **2003**, 107, 6170-6178.

Zhao, H.; Malhotra, S. V. "Applications of Ionic Liquids in Organic Synthesis" *Aldrichimica Acta*, 2002, 35, 75-83.

Zhu, L "Applications of Room Temperature Ionic Liquids in Interfacial Polymerization" Ph.D Dissertation, New Jersey Institute of Technology, Newark, NJ, 2006.